Functionally Altered Ruthenaindenes with Electron-rich and Electron-poor substituents

Hsiu L. Li,[†] Synøve Ø. Scottwell, James D. Watson,[†] Timothy E. Elton,[†] Hon C. Yu, Mohan Bhadbhade,[‡] Leslie D. Field,[†*]

[†] School of Chemistry, [‡] Mark Wainwright Analytical Centre, University of New South Wales, NSW 2052, Australia;

Supporting Information

CONTENTS

S1. COMPOUND NUMBERING

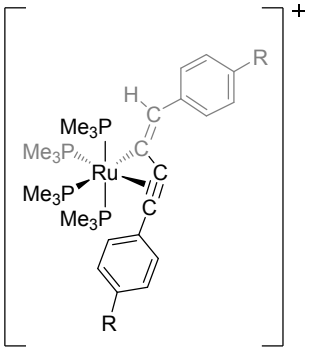

1a: R = OMe
1b: R = H
1c: R = CF_3

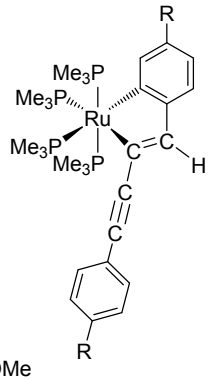

2a: R = OMe
2b: R = H
2c: R = CF_3

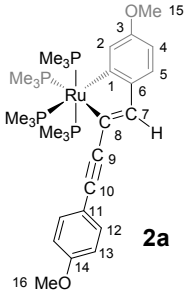

2a

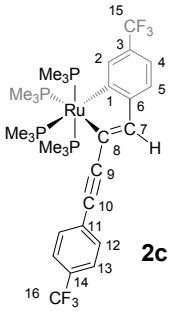

2c

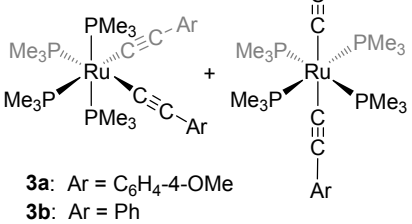

3a: Ar = C_6H_4-4-OMe
3b: Ar = Ph
3c: Ar = C_6H_4-4-CF_3

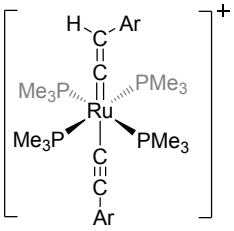

4a: Ar = C_6H_4-4-OMe
4b: Ar = Ph

S2. NMR AND HIGH RESOLUTION MASS SPECTRA

S2.1 [Ru(η³-MeO-4-C_6H_4C≡C-C=CH(C_6H_4-4-OMe))(PMe_3)$_4$]$^+$$BPh_4^-$ 1a-BPh_4.

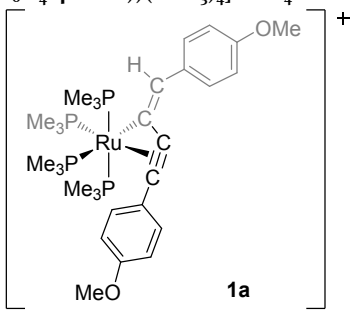

Figure S1. $^{31}P\{^1H\}$ NMR spectrum for [Ru(η³-MeO-4-C_6H_4C≡C-C=CH(C_6H_4-4-OMe))(PMe_3)$_4$]$^+$$BPh_4^-$ **1a-BPh_4** (acetone-d_6, 162 MHz)

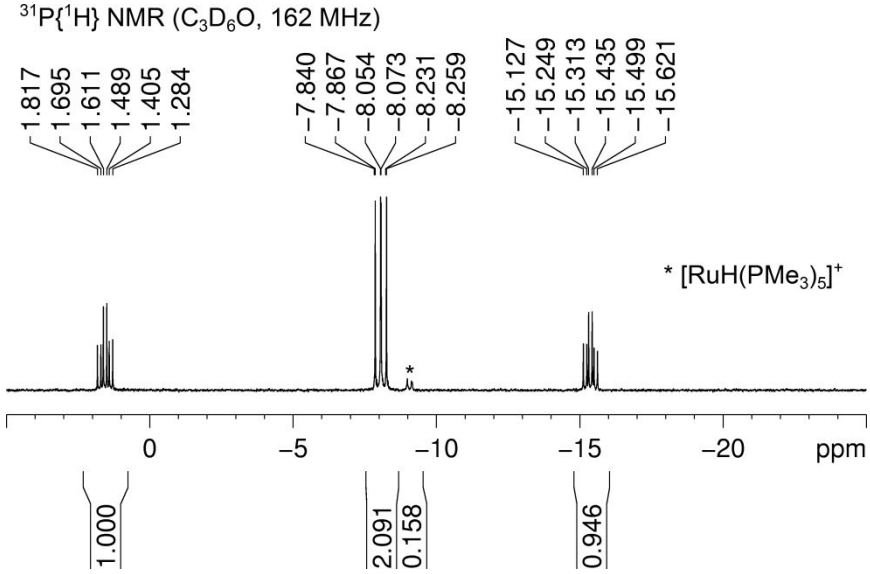

Figure S2. ^1H NMR spectrum for [Ru(η³-MeO-4-C_6H_4C≡C-C=CH(C_6H_4-4-OMe))(PMe_3)$_4$]$^+$$BPh_4^-$ **1a-BPh_4** (acetone-d_6, 400 MHz)

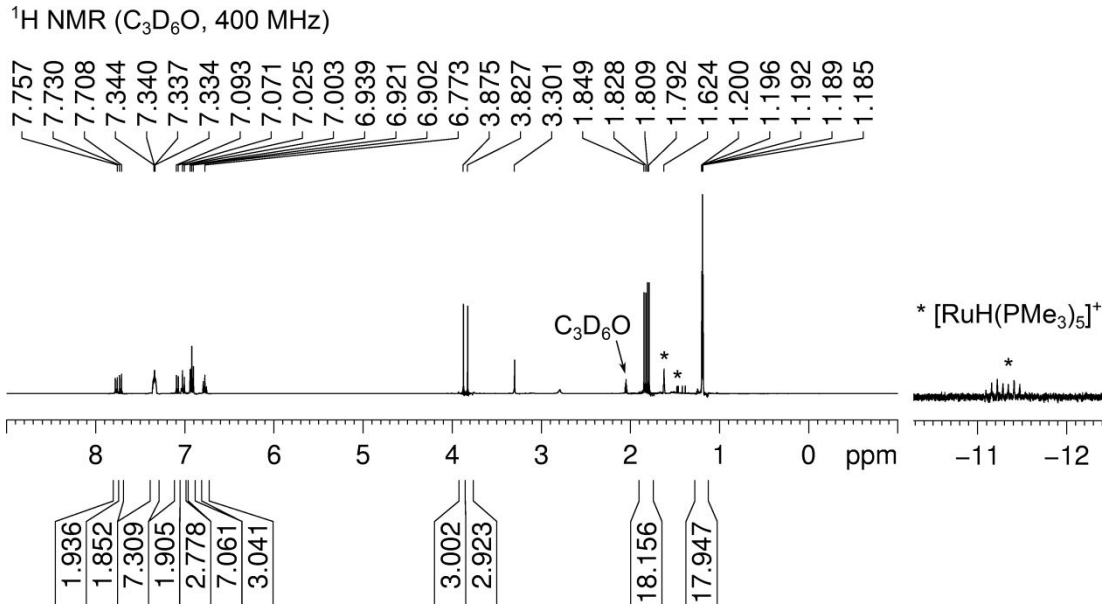

S2.2. [Ru(η³-MeO-4-C_6H_4C≡C-C=CH(C_6H_4-4-OMe))(PMe_3)$_4$]$^+BF_4^-$ 1a-BF_4.

Figure S3. $^{31}P\{^1H\}$ NMR spectrum for [Ru(η³-MeO-4-C_6H_4C≡C-C=CH(C_6H_4-4-OMe))(PMe_3)$_4$]$^+BF_4^-$ **1a-BF_4** (acetone-d_6, 243 MHz)

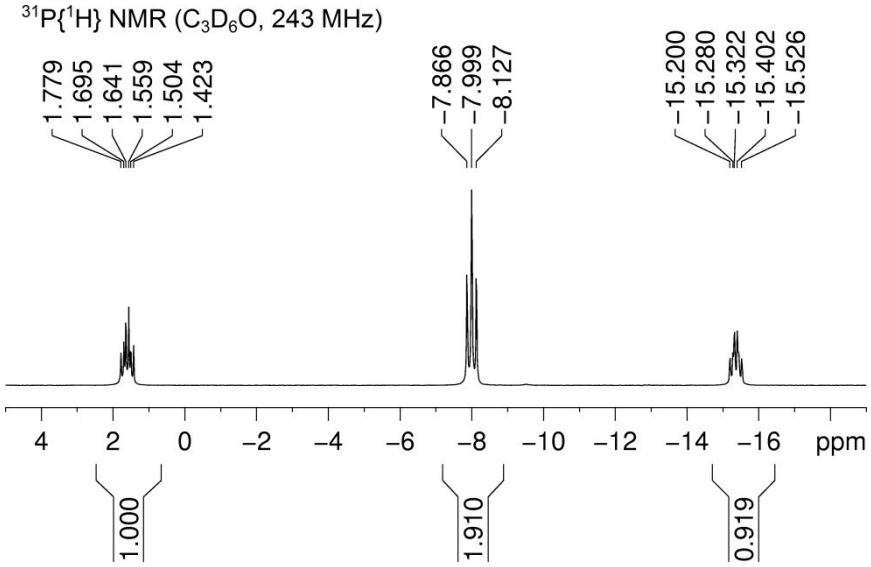

Figure S4. ^1H NMR spectrum for [Ru(η³-MeO-4-C_6H_4C≡C-C=CH(C_6H_4-4-OMe))(PMe_3)$_4$]$^+BF_4^-$ **1a-BF_4** (acetone-d_6, 600 MHz)

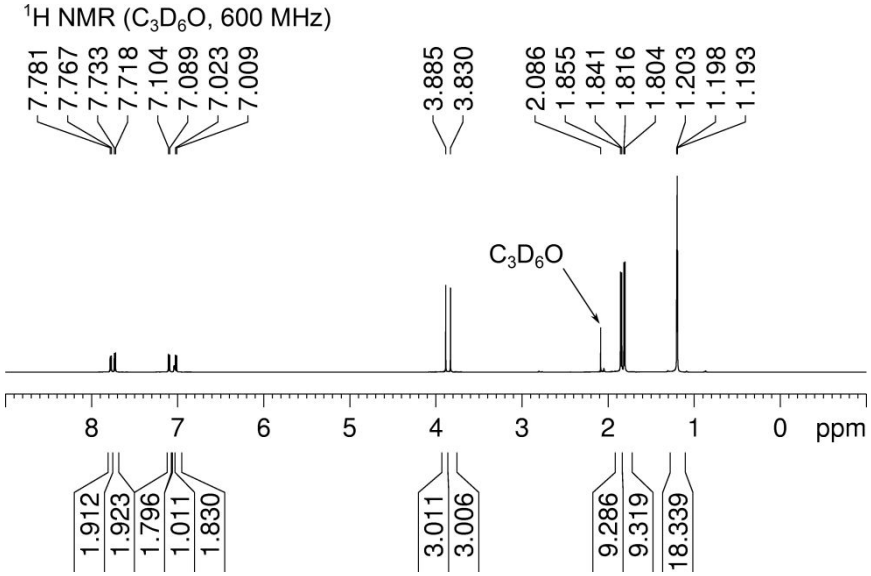

Figure S5. $^{13}C\{^{1}H\}$ NMR spectrum for $[Ru(\eta^3\text{-MeO-4-}C_6H_4C{\equiv}C\text{-}C{=}CH(C_6H_4\text{-4-OMe}))(PMe_3)_4]^+BF_4^-$ **1a-BF_4** (acetone-d_6, 151 MHz)

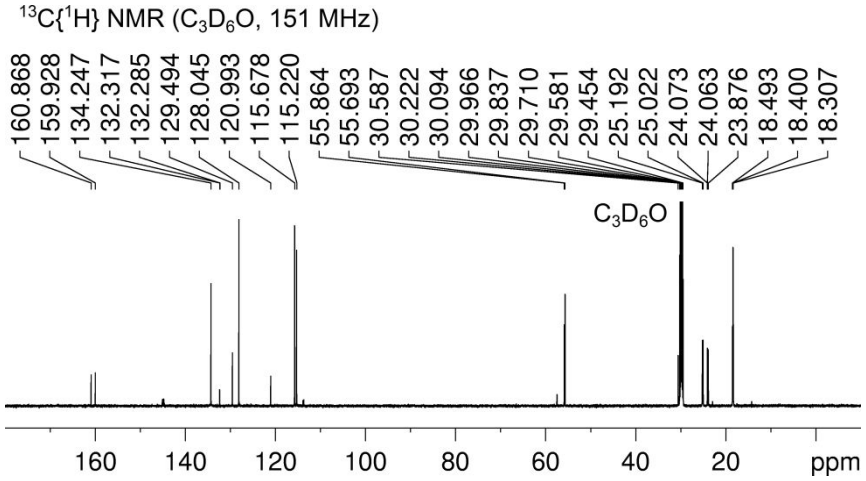

Figure S6. ^{19}F NMR spectrum for $[Ru(\eta^3\text{-MeO-4-}C_6H_4C{\equiv}C\text{-}C{=}CH(C_6H_4\text{-4-OMe}))(PMe_3)_4]^+BF_4^-$ **1a-BF_4** (acetone-d_6, 565 MHz)

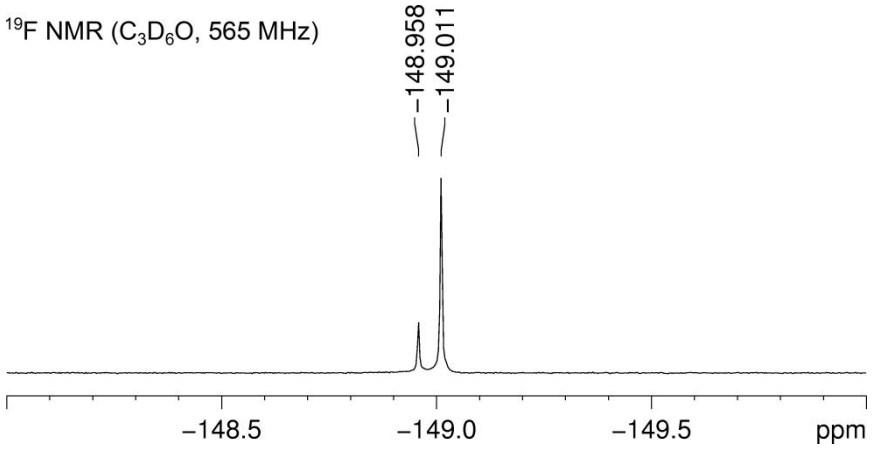

Figure S7. HRMS for [Ru(η³-MeO-4-C_6H_4C≡C-C=CH(C_6H_4-4-OMe))(PMe_3)$_4$]$^+BF_4^-$ **1a-BF_4** (acetonitrile, ESI)

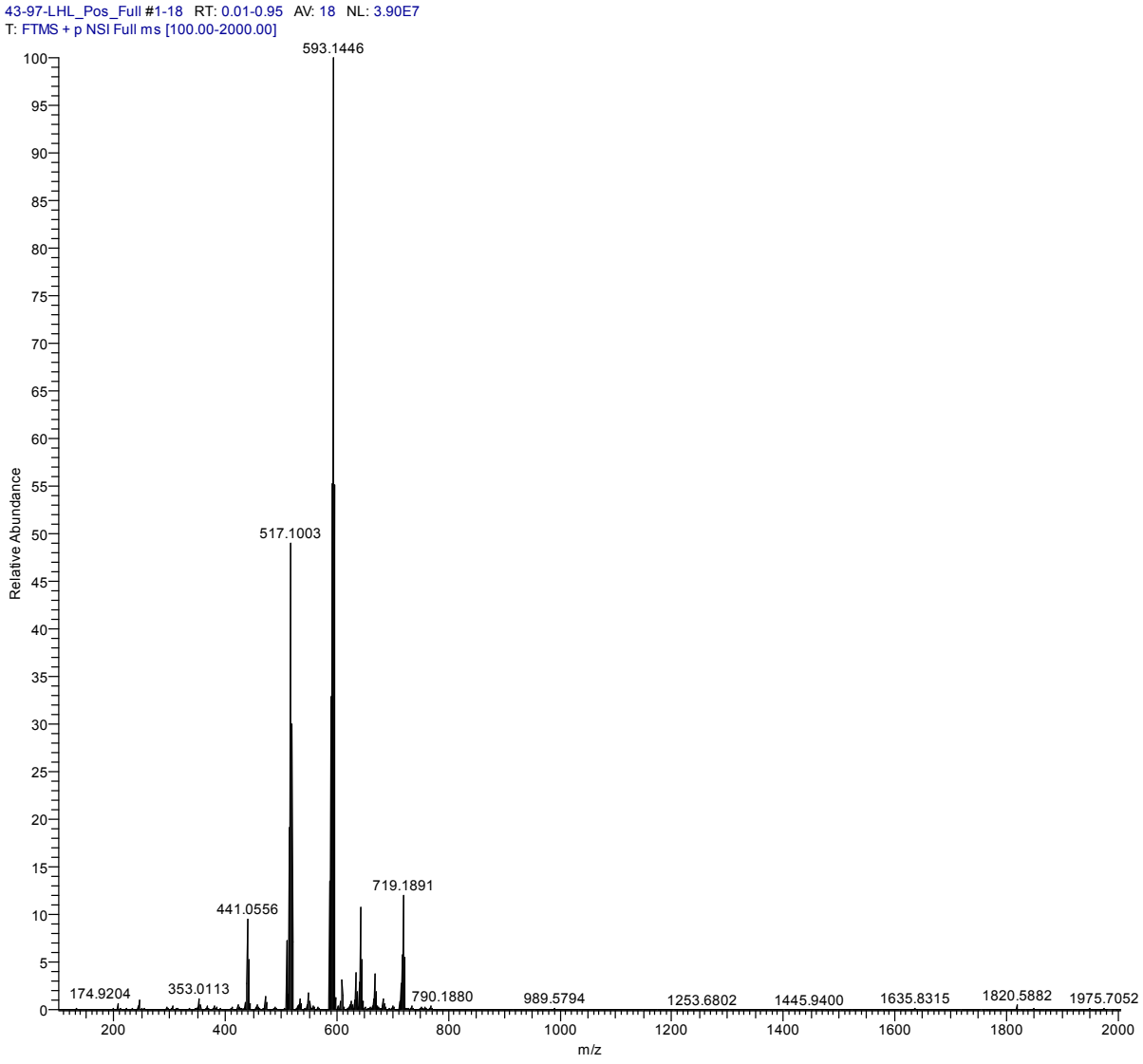

Figure S8. HRMS for [Ru(η³-MeO-4-C_6H_4C≡C-C=CH(C_6H_4-4-OMe))(PMe_3)$_4$]$^+BF_4^-$ **1a-BF_4** (expansion, acetonitrile, ESI)

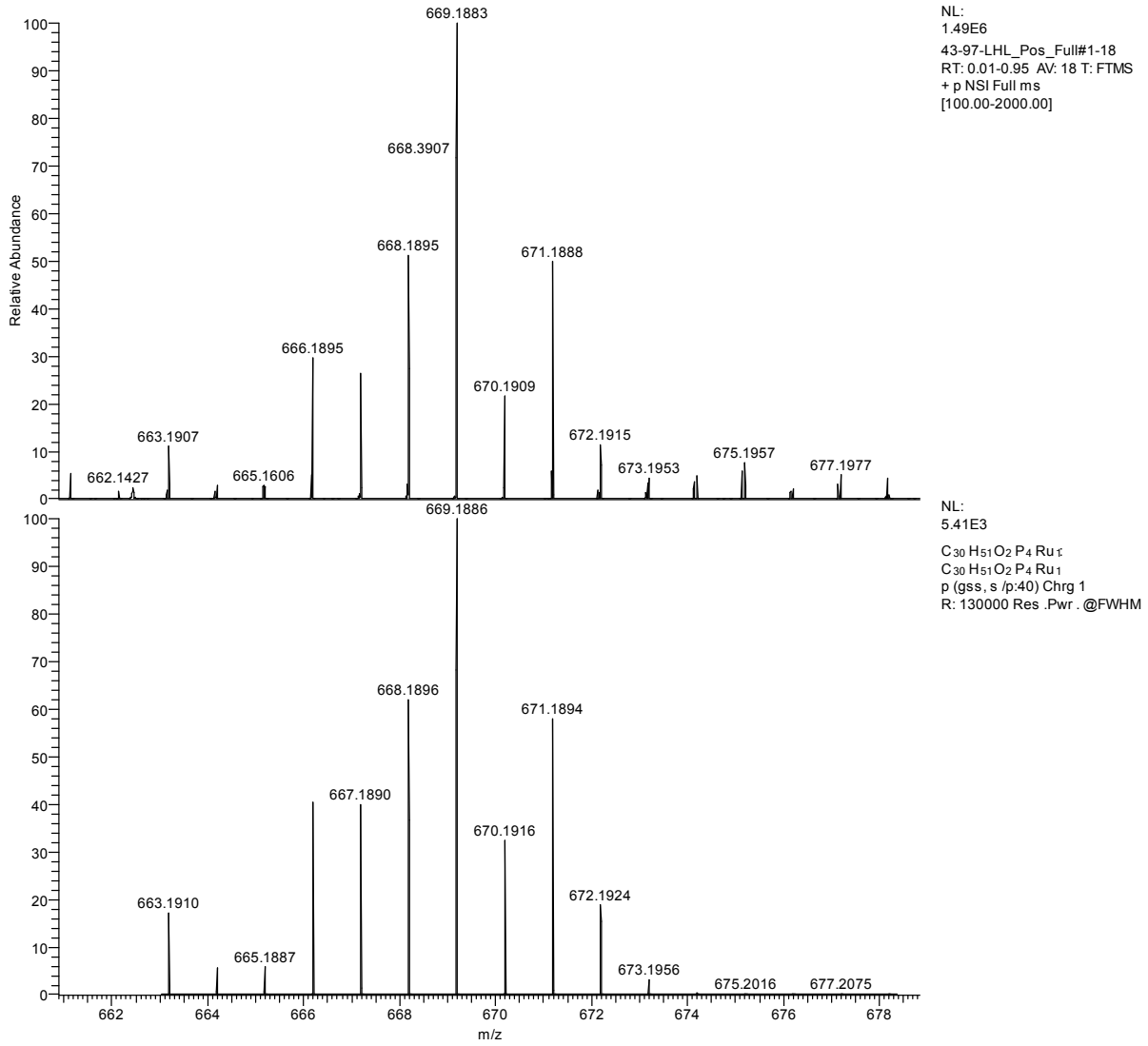

S2.3 [Ru(η³-PhC≡C-C=CH(Ph))(PMe$_3$)$_4$]$^+$BPh$_4^-$ 1b-BPh$_4$.

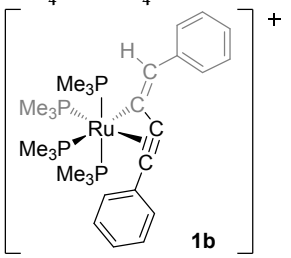

Figure S9. $^{31}P\{^1H\}$ NMR spectrum for [Ru(η³-PhC≡C-C=CH(Ph))(PMe$_3$)$_4$]$^+$BPh$_4^-$ **1b-BPh$_4$** (acetone-d_6, 243 MHz)

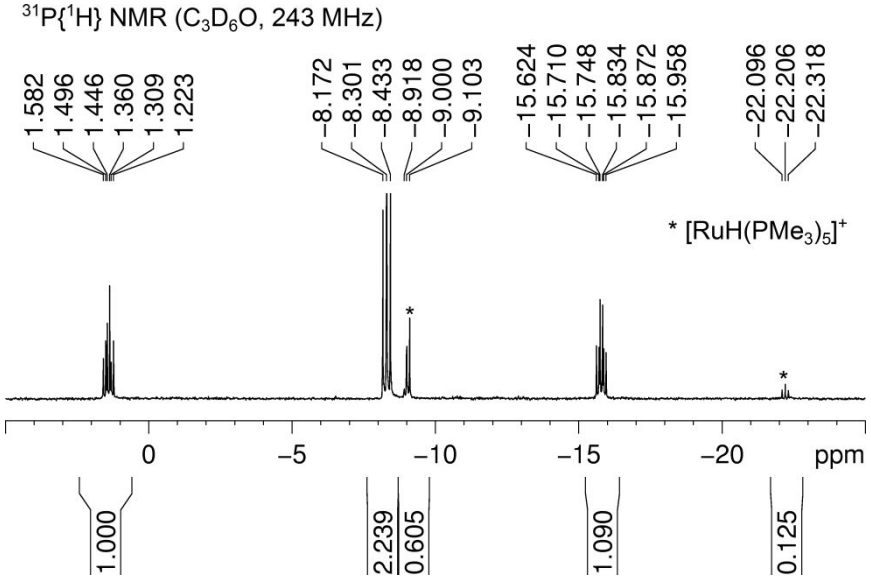

Figure S10. ^1H NMR spectrum for [Ru(η³-PhC≡C-C=CH(Ph))(PMe$_3$)$_4$]$^+$BPh$_4^-$ **1b-BPh$_4$** (acetone-d_6, 600 MHz)

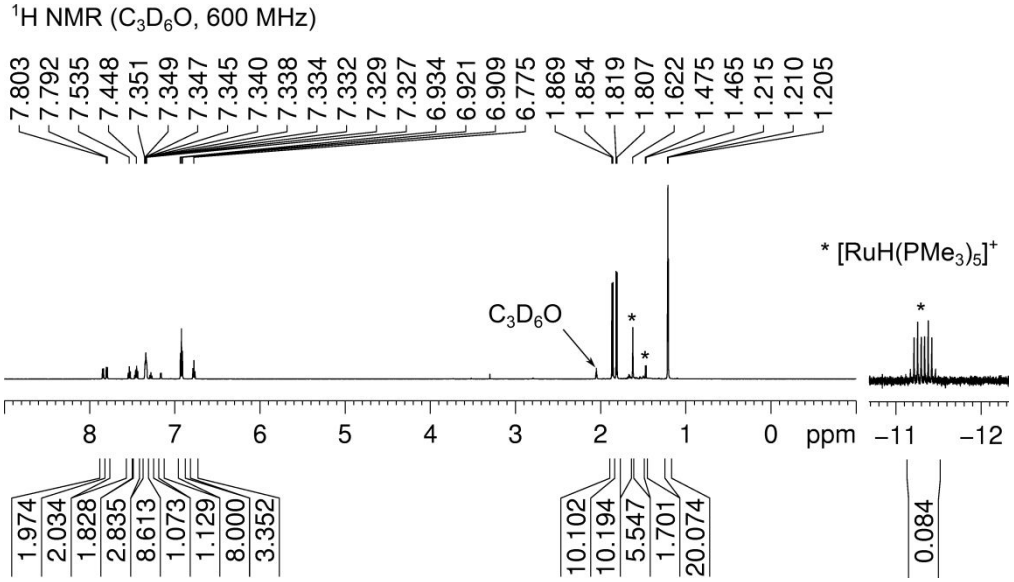

S2.4 [Ru(η³-CF_3-4-C_6H_4C≡C-C=CH(C_6H_4-4-CF_3))(PMe_3)$_4$]$^+$ BPh_4^- 1c-BPh_4.

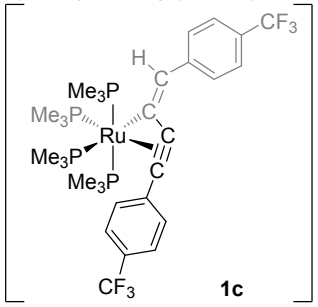

Figure S11. $^{31}P\{^1H\}$ NMR spectrum for [Ru(η³-CF_3-4-C_6H_4C≡C-C=CH(C_6H_4-4-CF_3))(PMe_3)$_4$]$^+$ BPh_4^- **1c-BPh$_4$** (acetone-d_6, 162 MHz)

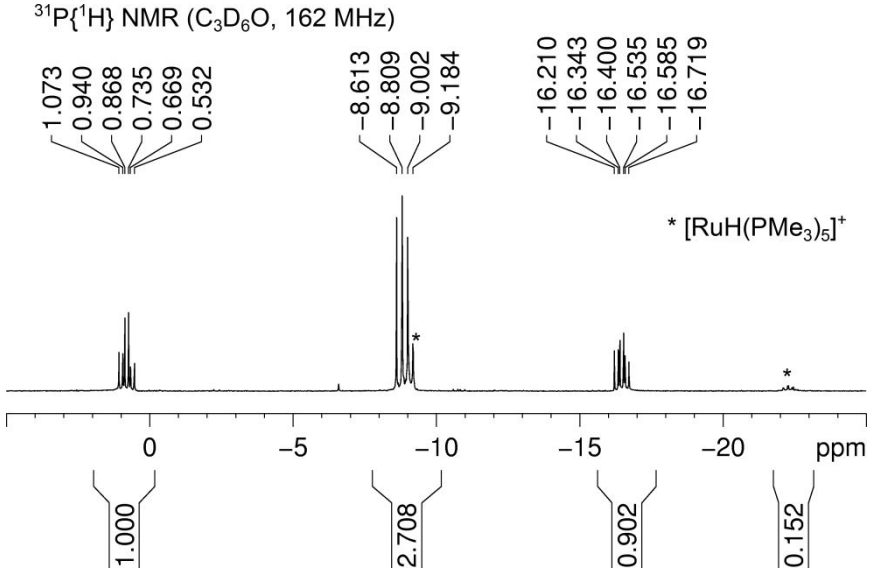

Figure S12. ^1H NMR spectrum for [Ru(η³-CF_3-4-C_6H_4C≡C-C=CH(C_6H_4-4-CF_3))(PMe_3)$_4$]$^+$ BPh_4^- **1c-BPh$_4$** (acetone-d_6, 400 MHz)

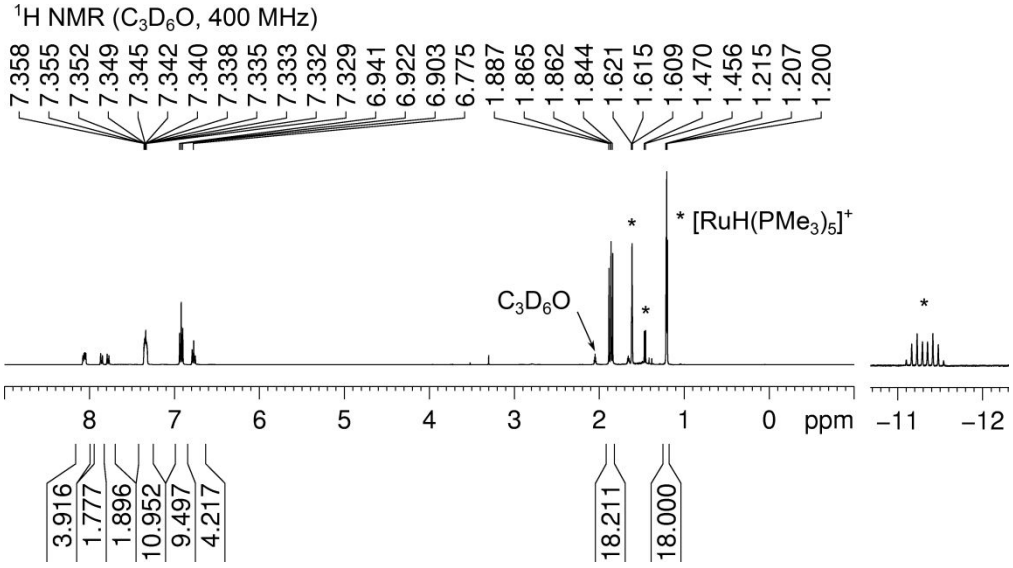

Figure S13. ^{19}F NMR spectrum for [Ru(η^3-CF_3-4-C_6H_4C≡C-C=CH(C_6H_4-4-CF_3))(PMe_3)$_4$]$^+$ BPh_4^- **1c-BPh$_4$** (acetone-d_6, 565 MHz)

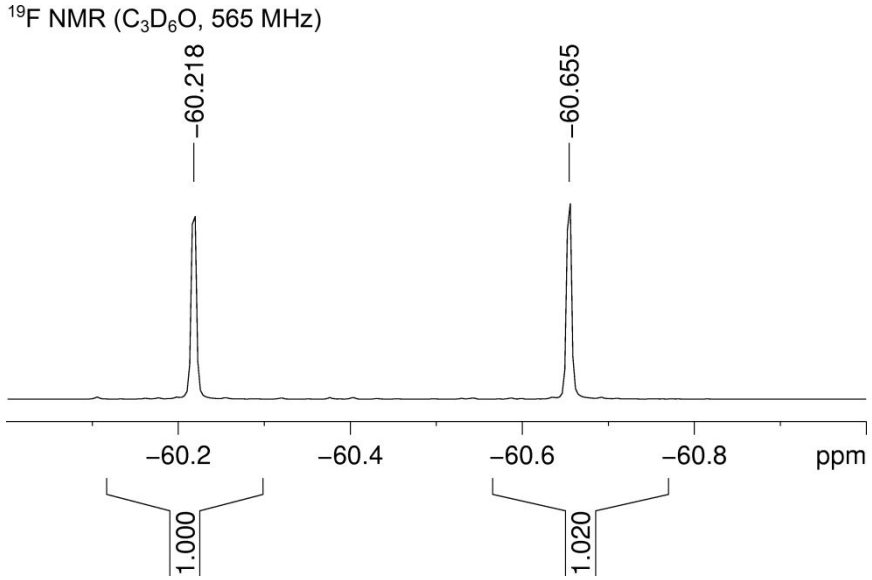

S2.5 [Ru(η^3-CF_3-4-C_6H_4C≡C-C=CH(C_6H_4-4-CF_3))(PMe_3)$_4$]$^+$ BF_4^- 1c-BF$_4$.

Figure S14. ^{31}P{^{1}H} NMR spectrum for [Ru(η^3-CF_3-4-C_6H_4C≡C-C=CH(C_6H_4-4-CF_3))(PMe_3)$_4$]$^+$ BF_4^- **1c-BF$_4$** (acetone-d_6, 162 MHz)

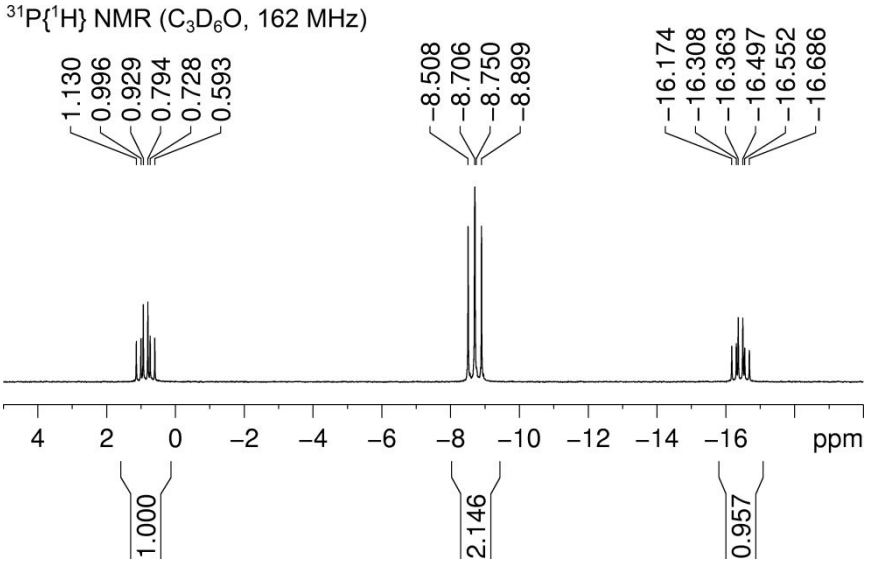

Figure S15. ^{1}H NMR spectrum for [Ru(η^{3}-CF_3-4-C_6H_4C≡C-C=CH(C_6H_4-4-CF_3))(PMe_3)$_4$]$^{+}$ BF_4^{-} **1c-BF_4** (acetone-d_6, 400 MHz)

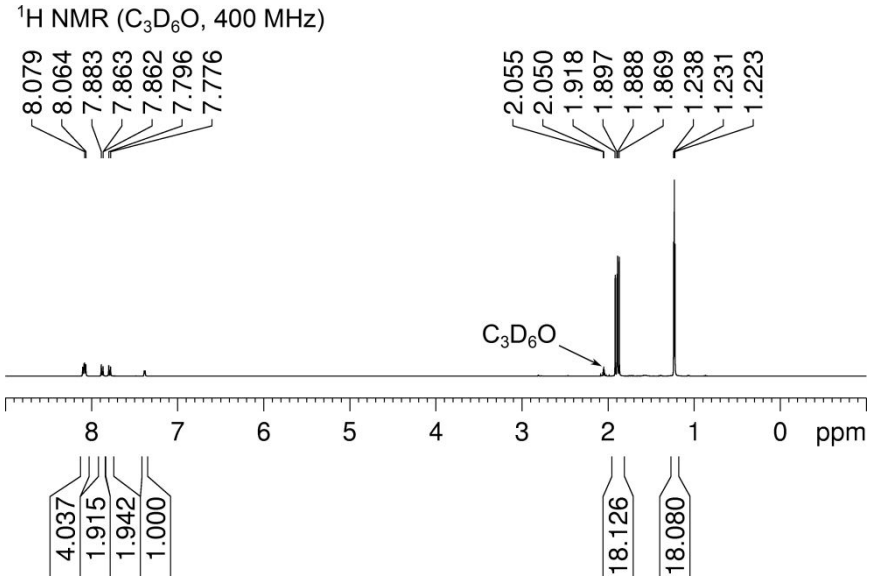

Figure S16. ^{13}C{^{1}H} NMR spectrum for [Ru(η^{3}-CF_3-4-C_6H_4C≡C-C=CH(C_6H_4-4-CF_3))(PMe_3)$_4$]$^{+}$ BF_4^{-} **1c-BF_4** (acetone-d_6, 101 MHz)

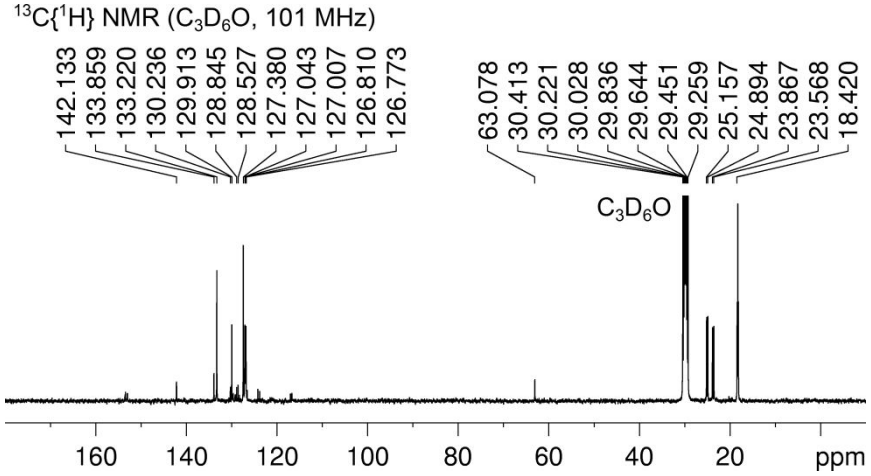

Figure S17. ^{19}F NMR spectrum for [Ru(η^3-CF_3-4-C_6H_4C≡C-C=CH(C_6H_4-4-CF_3))(PMe_3)$_4$]$^+$ BF_4^- **1c-BF_4** (acetone-d_6, 376 MHz)

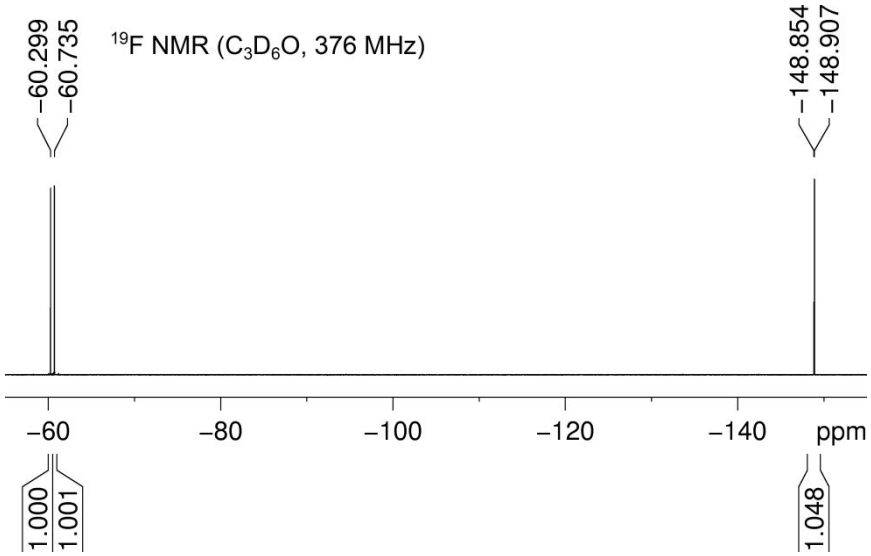

S2.6 [Ru(C(C≡CC_6H_4-4-OMe)=CH(C_6H_3-4-OMe)(PMe_3)$_4$] 2a.

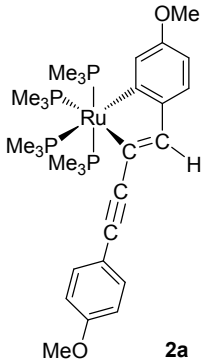

2a

Figure S18. $^{31}P\{^1H\}$ NMR spectrum for [Ru(C(C≡CC_6H_4-4-OMe)=CH(C_6H_3-4-OMe)(PMe_3)$_4$] **2a** (tetrahydrofuran-d_8, 162 MHz)

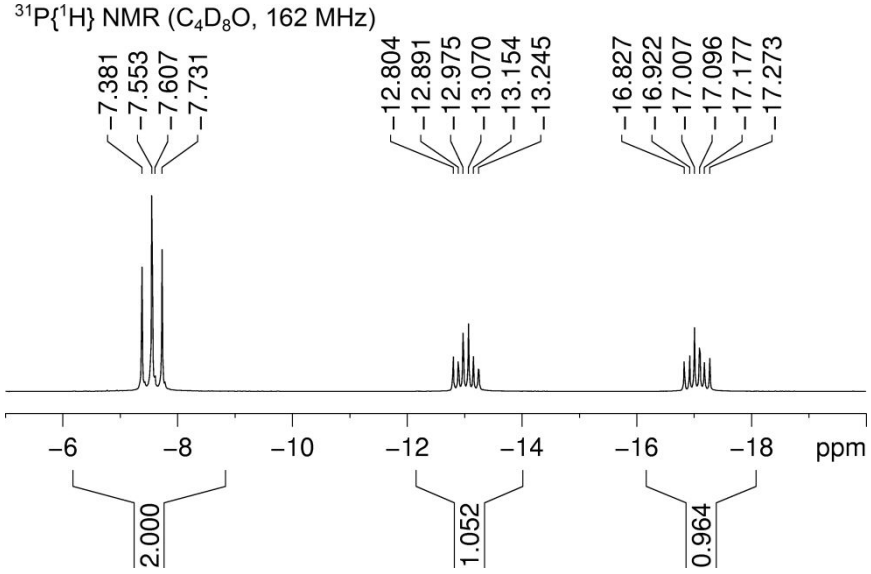

Figure S19. ^{1}H NMR spectrum for [Ru(C(C≡CC_6H_4-4-OMe)=CH(C_6H_3-4-OMe)(PMe_3)$_4$] **2a** (tetrahydrofuran-d_8, 400 MHz)

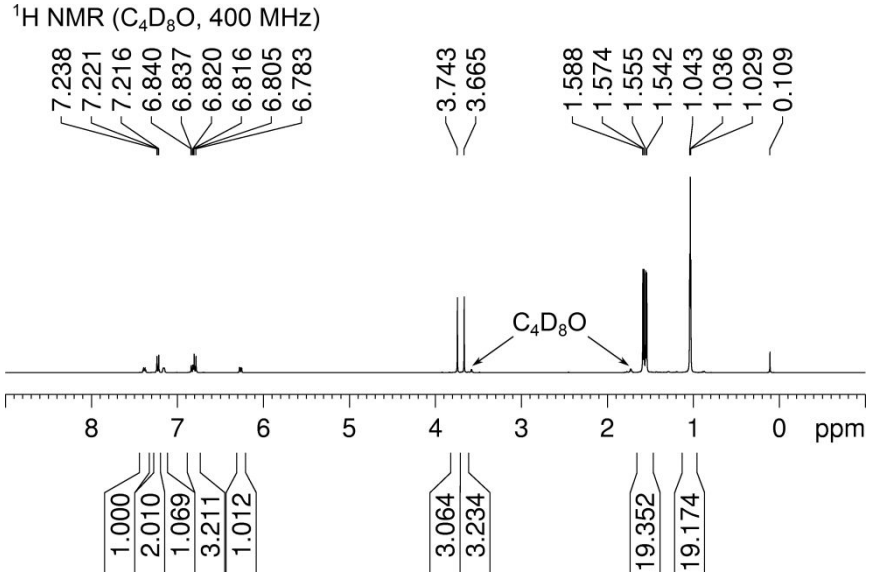

Figure S20. ^{13}C{^{1}H} NMR spectrum for [Ru(C(C≡CC_6H_4-4-OMe)=CH(C_6H_3-4-OMe)(PMe_3)$_4$] **2a** (tetrahydrofuran-d_8, 101 MHz)

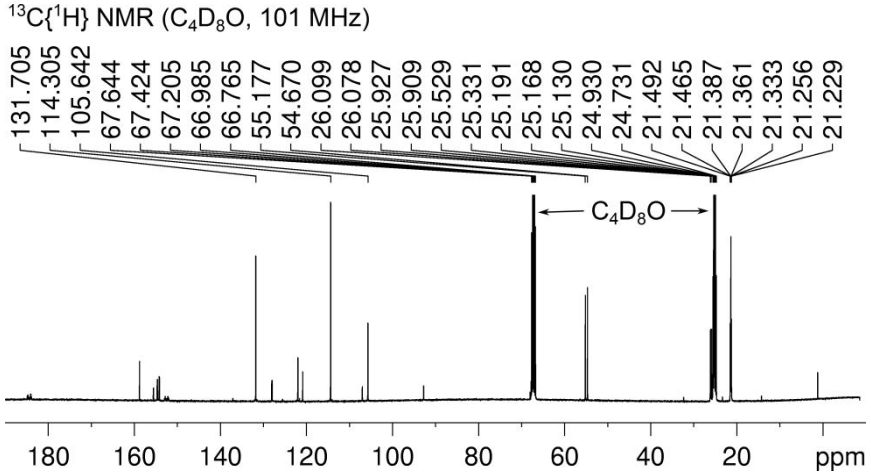

Figure S21. HRMS for [Ru(C(C≡CC$_6$H$_4$-4-OMe)=CH(C$_6$H$_3$-4-OMe)(PMe$_3$)$_4$] 2a (acetonitrile, ESI)

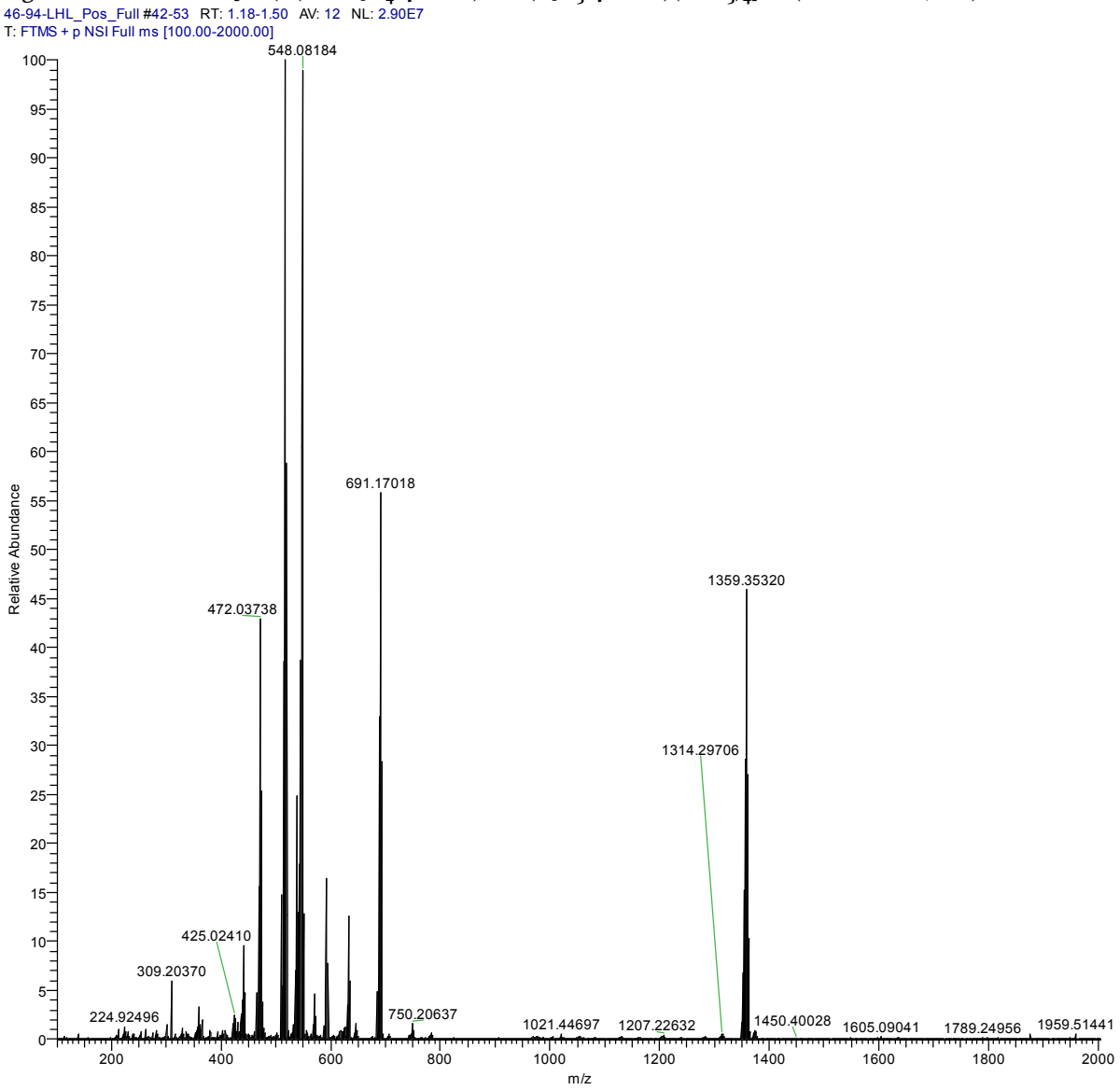

Figure S22. HRMS for [Ru(C(C≡CC$_6$H$_4$-4-OMe)=CH(C$_6$H$_3$-4-OMe)(PMe$_3$)$_4$] 2a (expansion, acetonitrile, ESI)

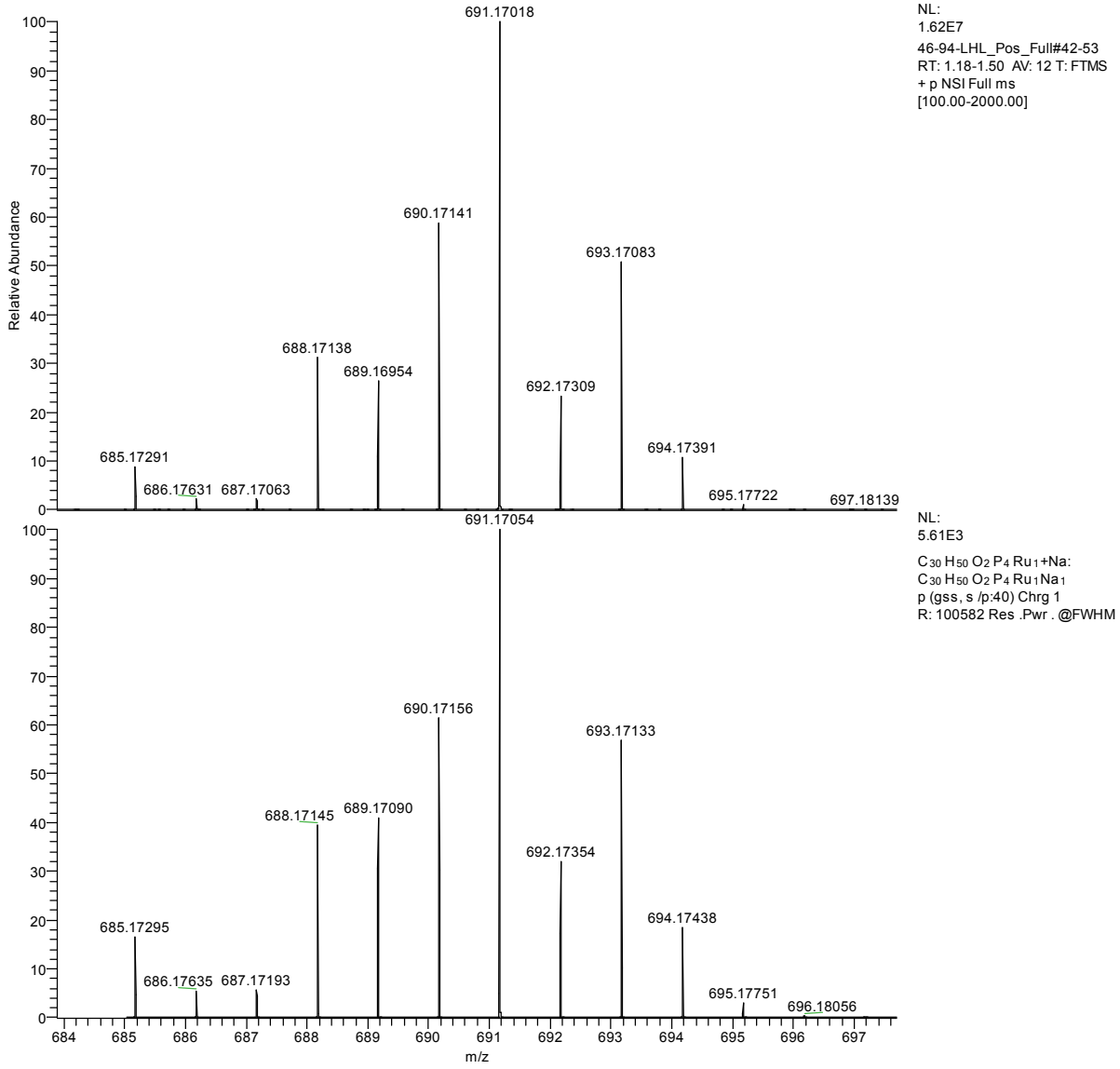

S2.7 [Ru(CF_3-4-C_6H_4C≡C-C=CH(C_6H_3-4-CF_3)(PMe_3)$_4$] 2c.

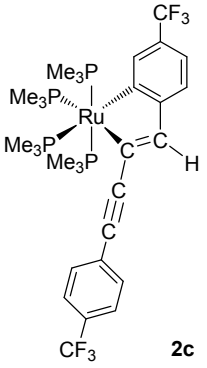

2c

Figure S23. $^{31}P\{^1H\}$ NMR spectrum for [Ru(CF_3-4-C_6H_4C≡C-C=CH(C_6H_3-4-CF_3)(PMe_3)$_4$] **2c** (tetrahydrofuran-d_8, 243 MHz)

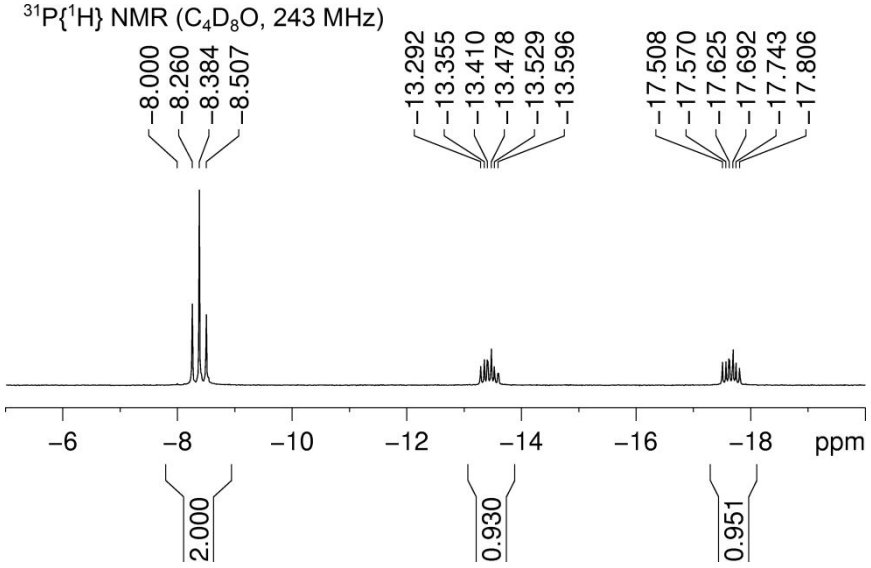

Figure S24. ^1H NMR spectrum for [Ru(CF_3-4-C_6H_4C≡C-C=CH(C_6H_3-4-CF_3)(PMe_3)$_4$] **2c** (tetrahydrofuran-d_8, 600 MHz)

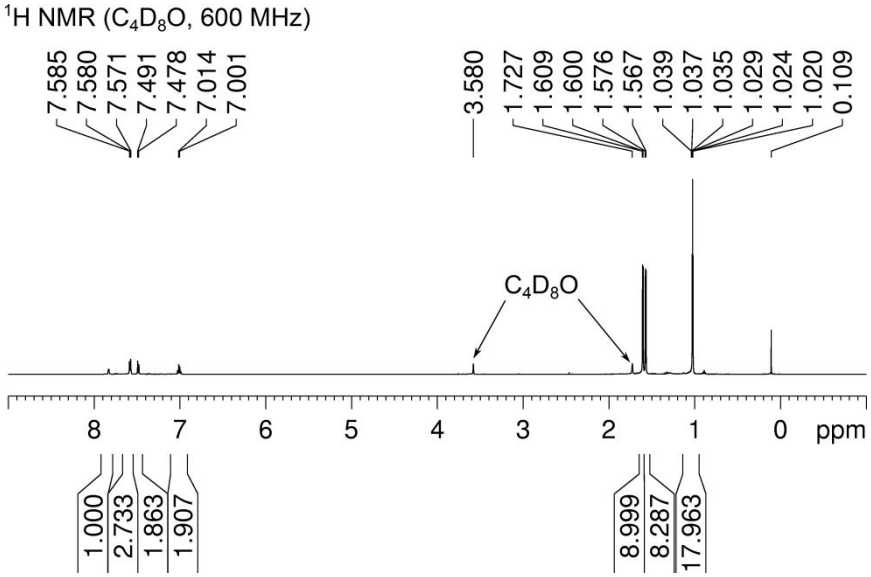

Figure S25. $^{13}C\{^{1}H\}$ NMR spectrum for [Ru(CF_3-4-C_6H_4C≡C-C=CH(C_6H_3-4-CF_3)(PMe_3)$_4$] **2c** (tetrahydrofuran-d_8, 151 MHz)

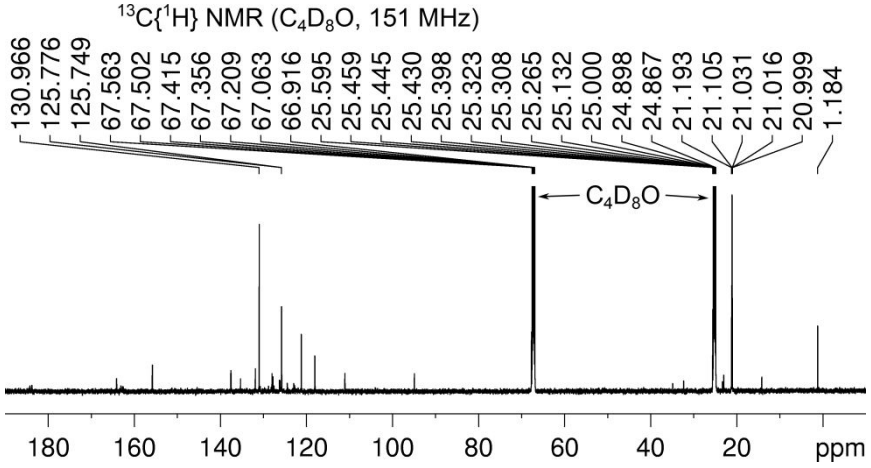

Figure S26. ^{19}F NMR spectrum for [Ru(CF_3-4-C_6H_4C≡C-C=CH(C_6H_3-4-CF_3)(PMe_3)$_4$] **2c** (tetrahydrofuran-d_8, 565 MHz)

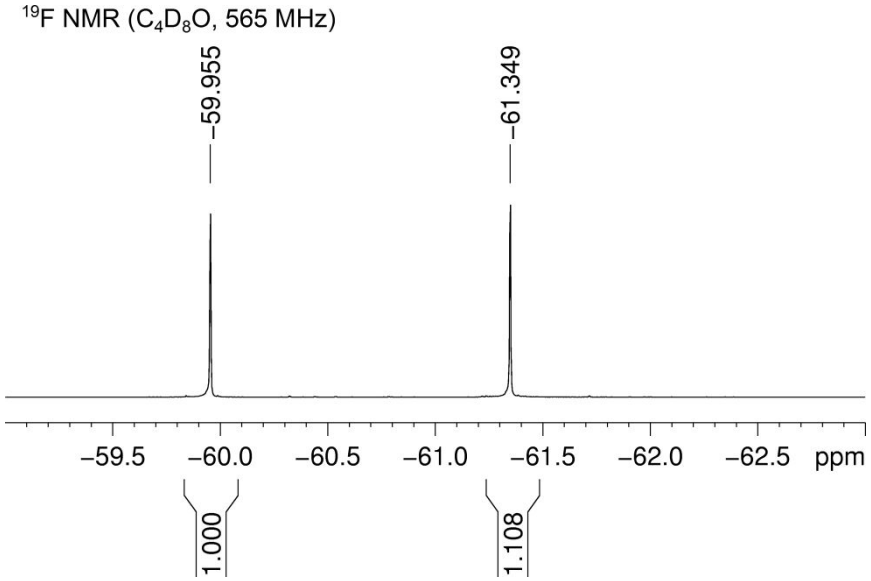

Figure S27. HRMS for [Ru(CF_3-4-C_6H_4C≡C-C=CH(C_6H_3-4-CF_3)(PMe_3)$_4$] 2c (acetonitrile, ESI)

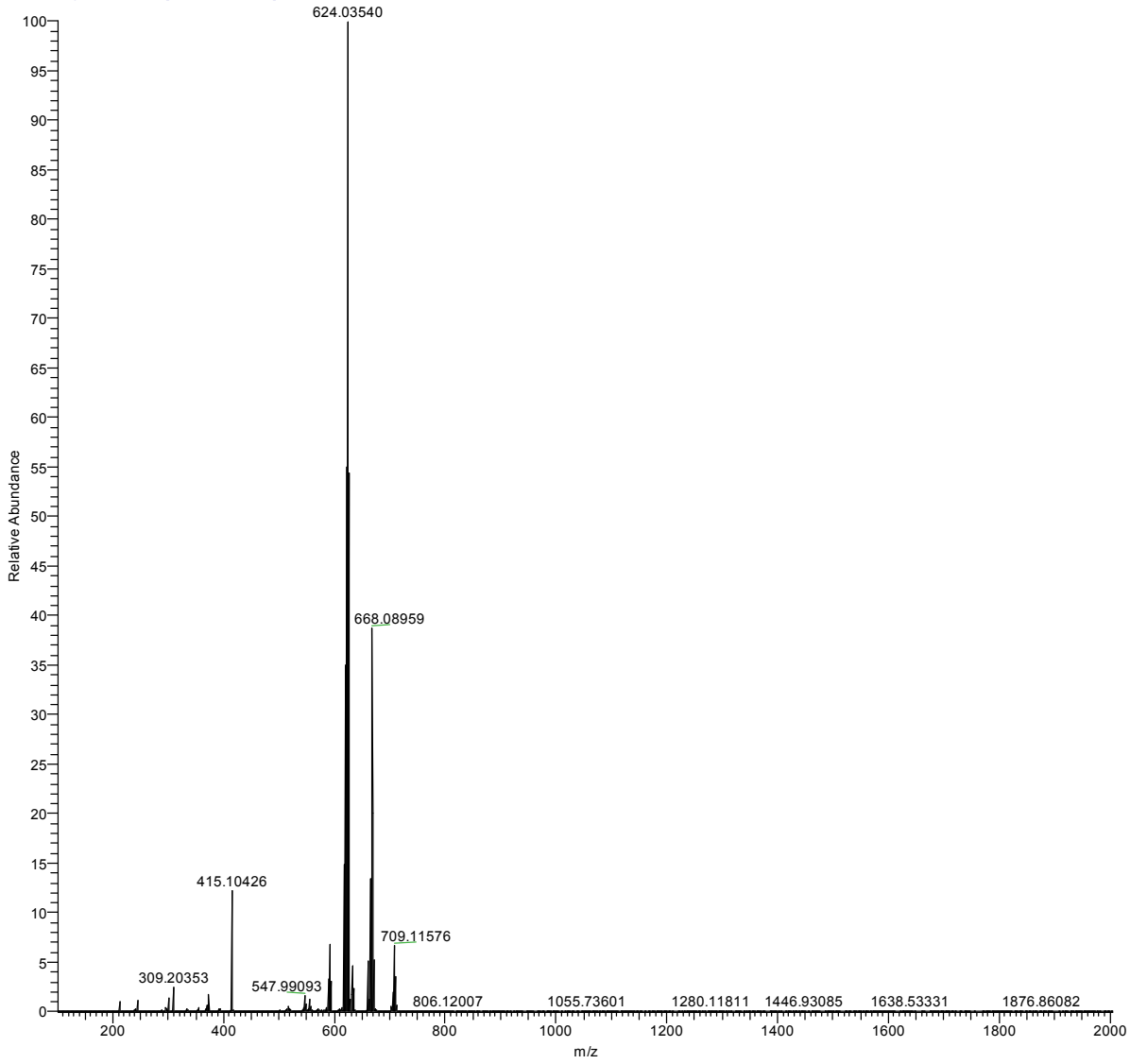

Figure S28. HRMS for [Ru(CF_3-4-C_6H_4C≡C-C=CH(C_6H_3-4-CF_3)(PMe_3)$_4$] 2c (expansion, acetonitrile, ESI)

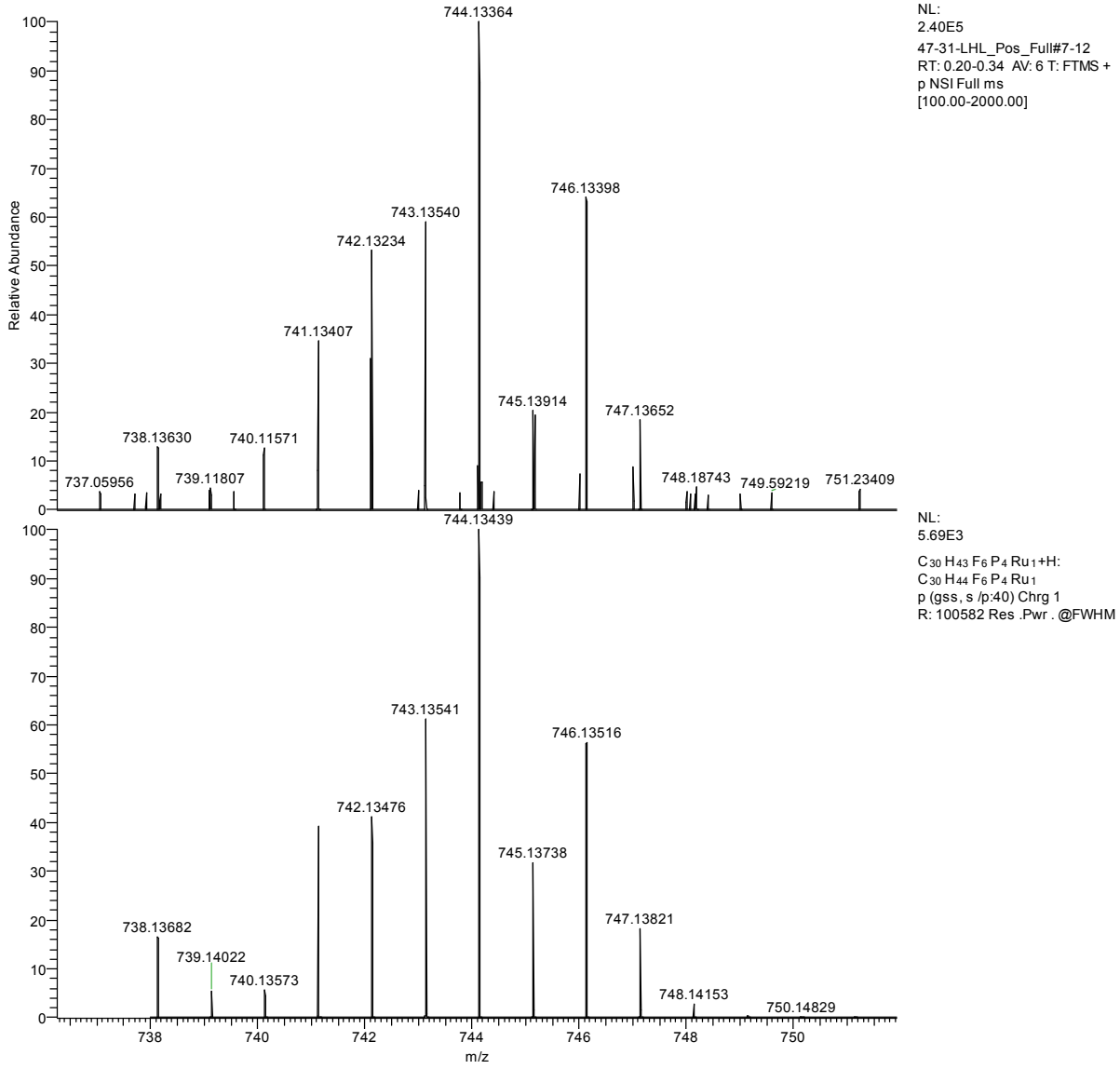

S2.8 ***cis*/*trans*-[Ru(C≡CC$_6$H$_4$-4-OMe)$_2$(PMe$_3$)$_4$] 3a.**

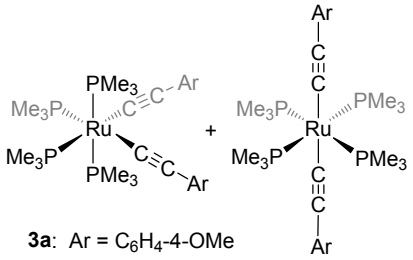

Figure S29. $^{31}P\{^1H\}$ NMR spectrum for *cis*/*trans*-[Ru(C≡CC$_6$H$_4$-4-OMe)$_2$(PMe$_3$)$_4$] **3a** (tetrahydrofuran-d_8, 162 MHz)

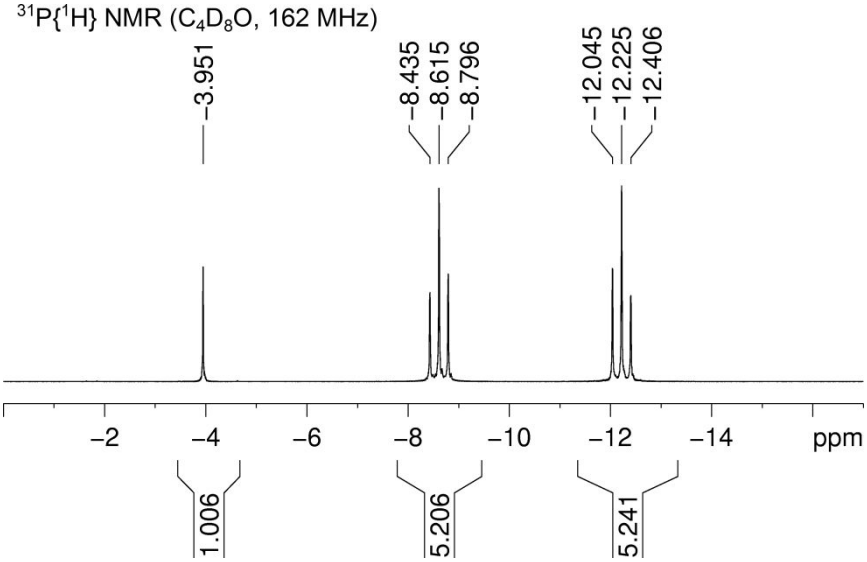

Figure S30. ^1H NMR spectrum for *cis*/*trans*-[Ru(C≡CC$_6$H$_4$-4-OMe)$_2$(PMe$_3$)$_4$] **3a** (tetrahydrofuran-d_8, 400 MHz)

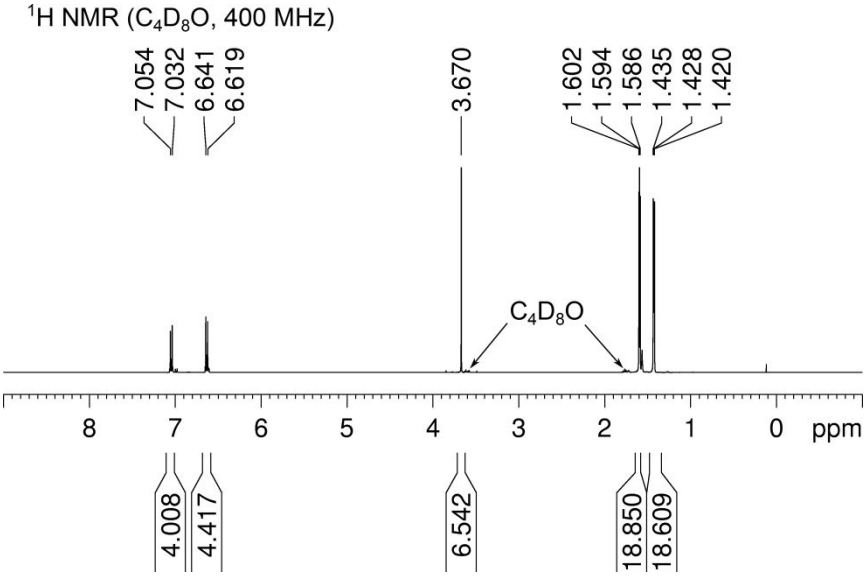

Figure S31. $^{13}C\{^{1}H\}$ NMR spectrum for *cis*/*trans*-[Ru(C≡CC_6H_4-4-OMe)$_2$(PMe_3)$_4$] **3a** (tetrahydrofuran-d_8, 101 MHz)

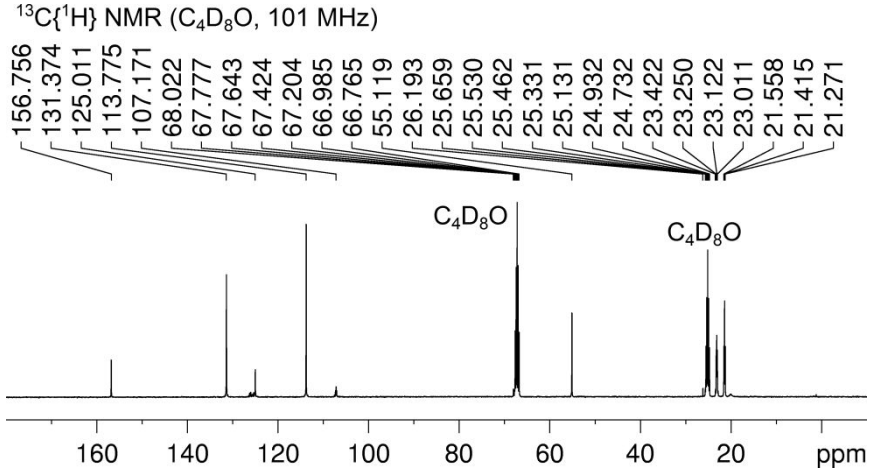

Figure S32. HRMS for *cis*/*trans*-[Ru(C≡CC_6H_4-4-OMe)$_2$(PMe_3)$_4$] 3a (acetonitrile, ESI)

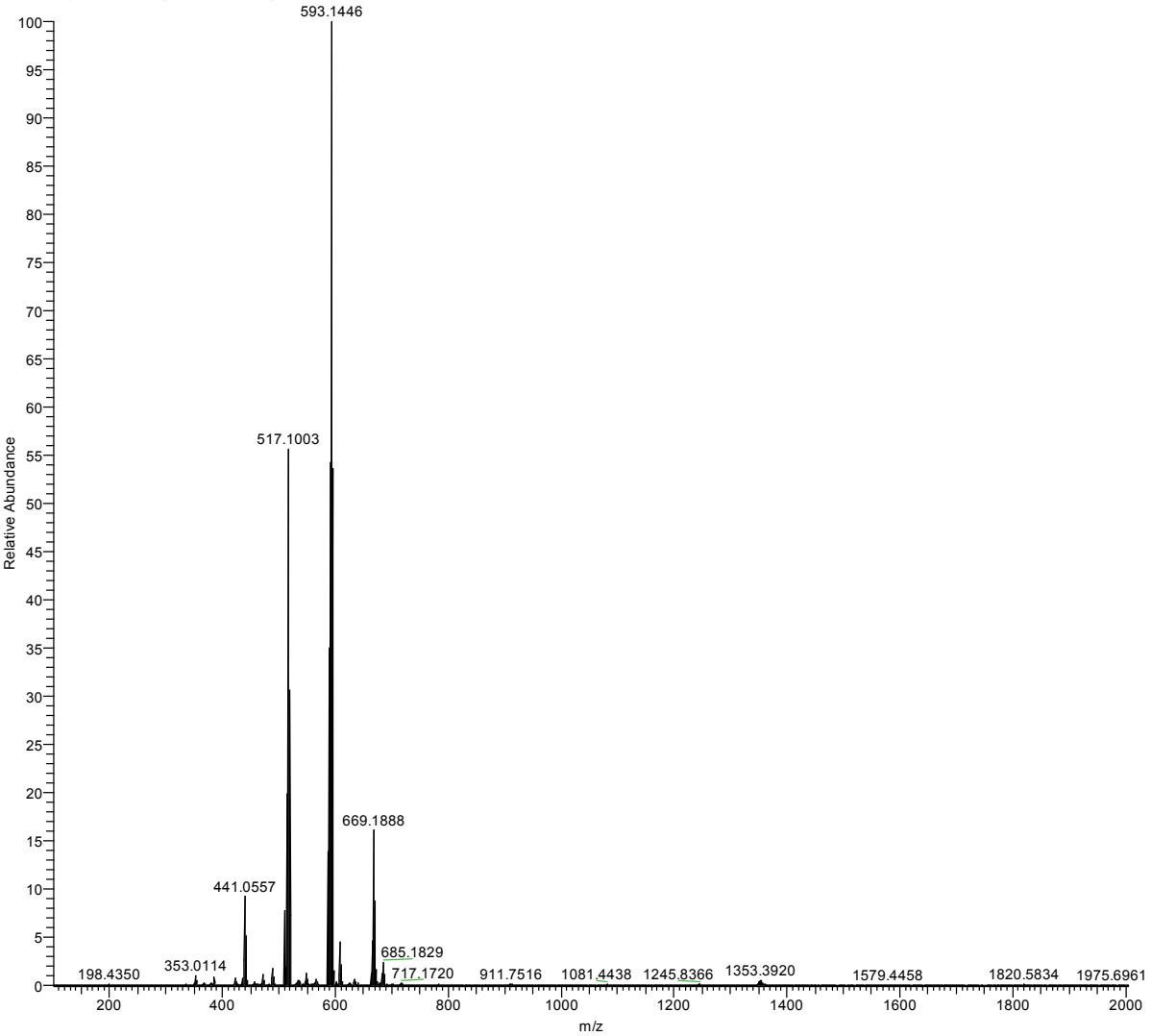

Figure S33. HRMS for *cis*/*trans*-[Ru(C≡CC_6H_4-4-OMe)$_2$(PMe_3)$_4$] 3a (expansion, acetonitrile, ESI)

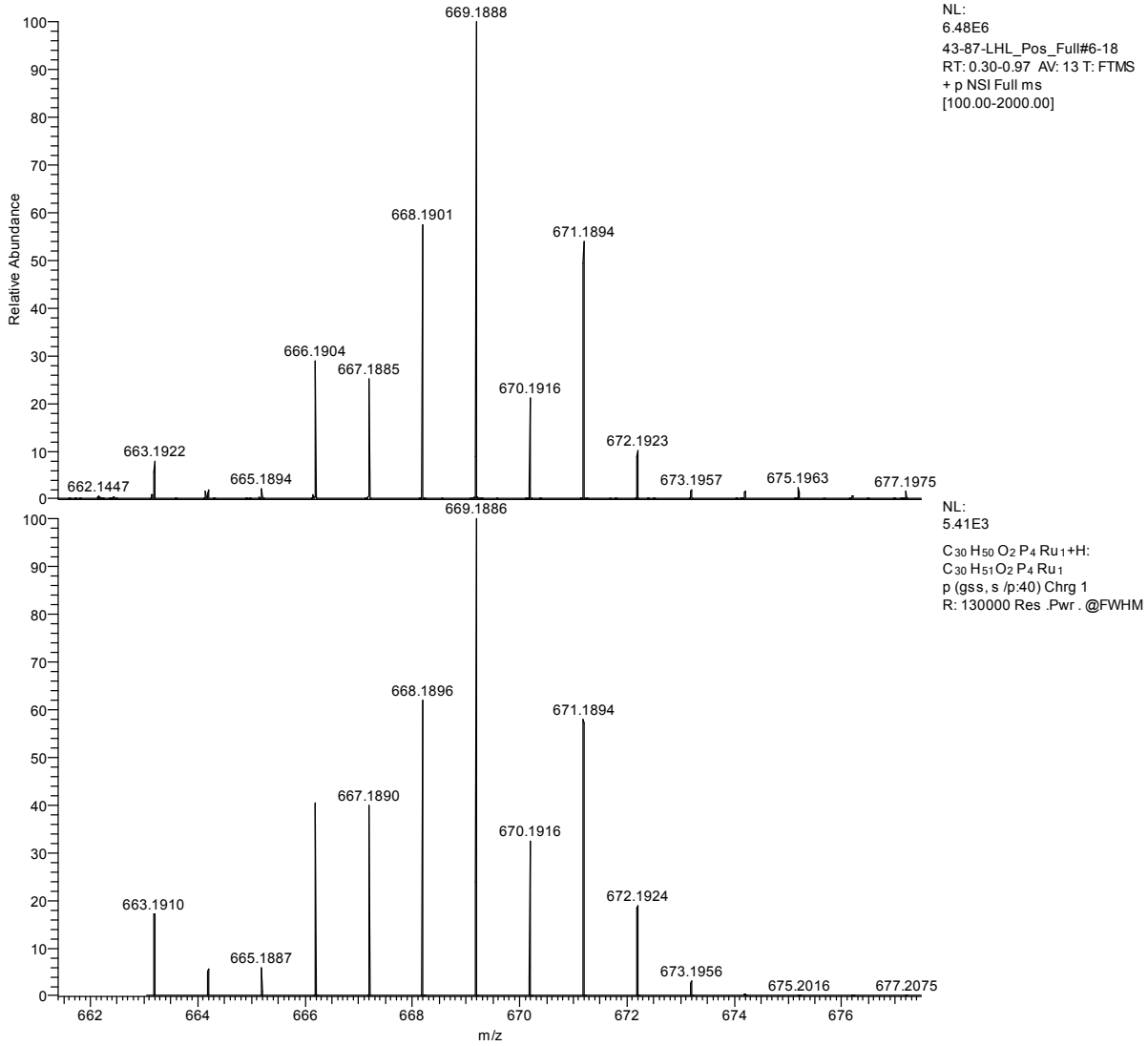

S2.9 ***cis*/*trans*-[Ru(C≡CC$_6$H$_4$-4-CF$_3$)$_2$(PMe$_3$)$_4$] 3c.**

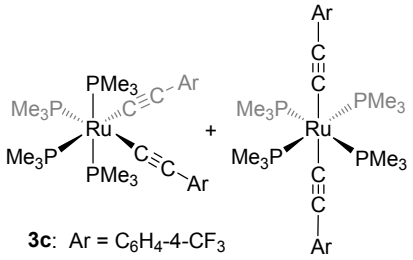

Figure S34. $^{31}P\{^1H\}$ NMR spectrum for *cis*/*trans*-[Ru(C≡CC$_6$H$_4$-4-CF$_3$)$_2$(PMe$_3$)$_4$] **3c** (benzene-d_6, 162 MHz)

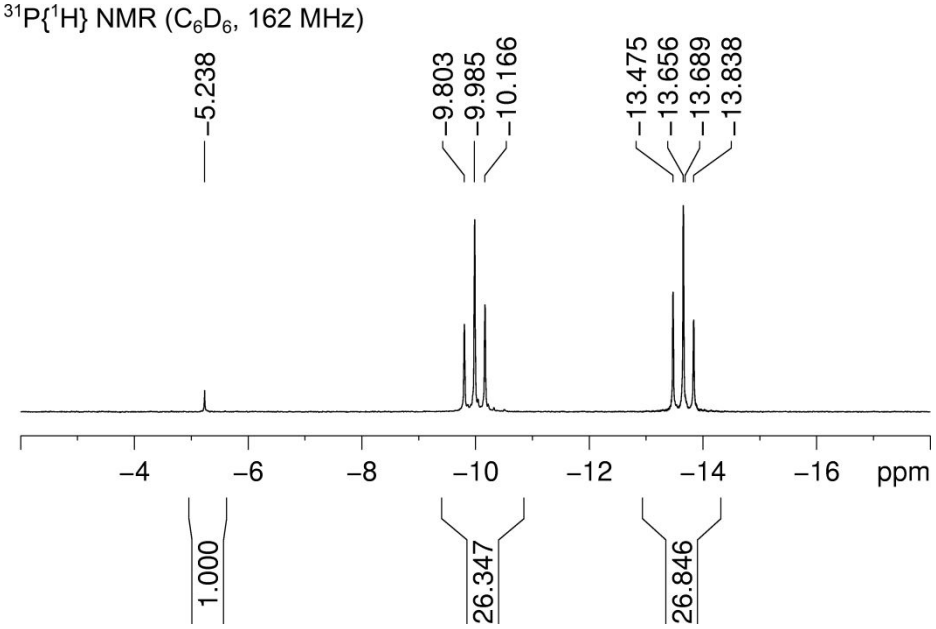

Figure S35. ^1H NMR spectrum for *cis*/*trans*-[Ru(C≡CC$_6$H$_4$-4-CF$_3$)$_2$(PMe$_3$)$_4$] **3c** (benzene-d_6, 400 MHz)

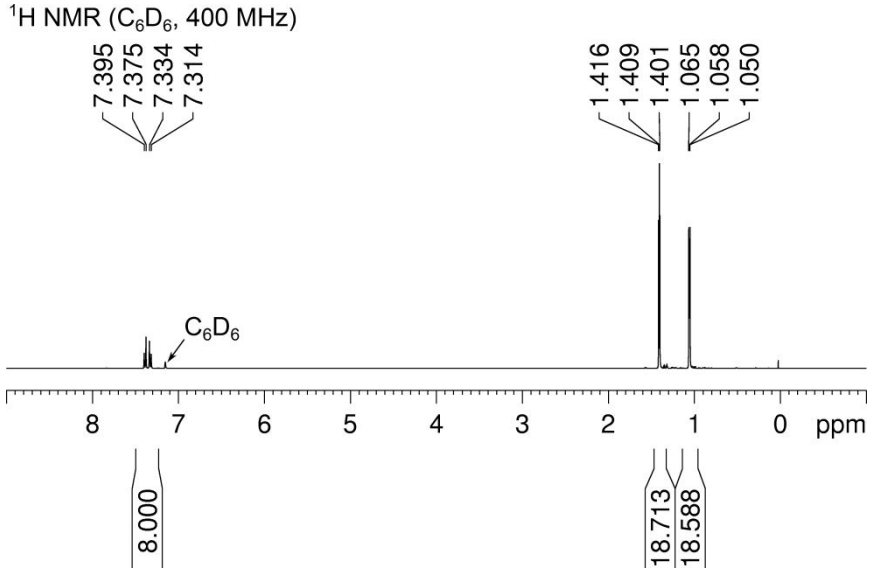

Figure S36. $^{13}C\{^{1}H\}$ NMR spectrum for *cis*/*trans*-[Ru(C≡CC_6H_4-4-CF_3)$_2$(PMe_3)$_4$] **3c** (benzene-d_6, 101 MHz)

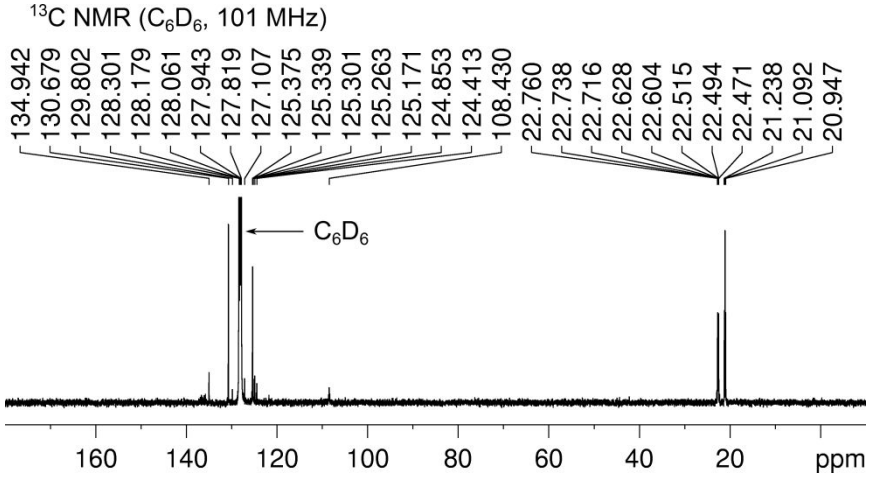

Figure S37. ^{19}F NMR spectrum for *cis*/*trans*-[Ru(C≡CC_6H_4-4-CF_3)$_2$(PMe_3)$_4$] **3c** (benzene-d_6, 376 MHz)

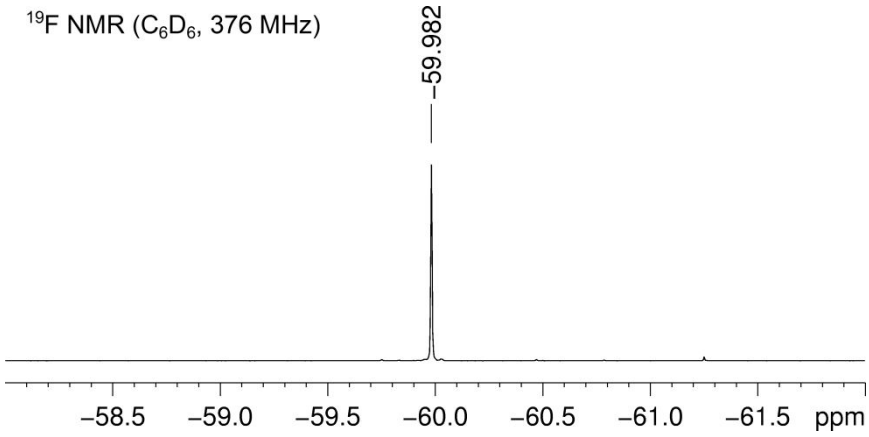

S2.10 ***Trans*-[Ru(=C=CH(C_6H_4-4-OMe))(C≡CC_6H_4-4-OMe)(PMe_3)$_4$]$^+$ BF_4^- 4a.**

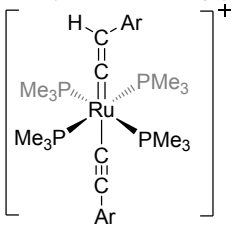

4a: Ar = C_6H_4-4-OMe

Figure S38. $^{31}P\{^1H\}$ NMR spectrum for *trans*-[Ru(=C=CH(C_6H_4-4-OMe))(C≡CC_6H_4-4-OMe)(PMe_3)$_4$]$^+$ BF_4^- **4a** (acetone-d_6, 162 MHz)

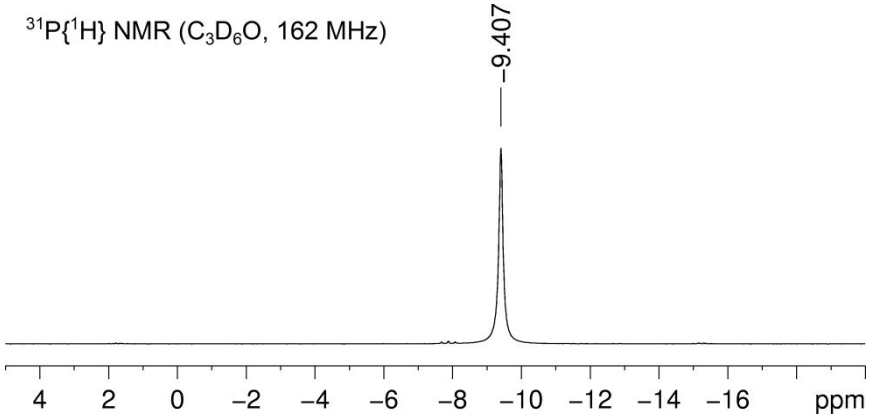

Figure S39. ^1H NMR spectrum for *trans*-[Ru(=C=CH(C_6H_4-4-OMe))(C≡CC_6H_4-4-OMe)(PMe_3)$_4$]$^+$ BF_4^- **4a** (acetone-d_6, 400 MHz)

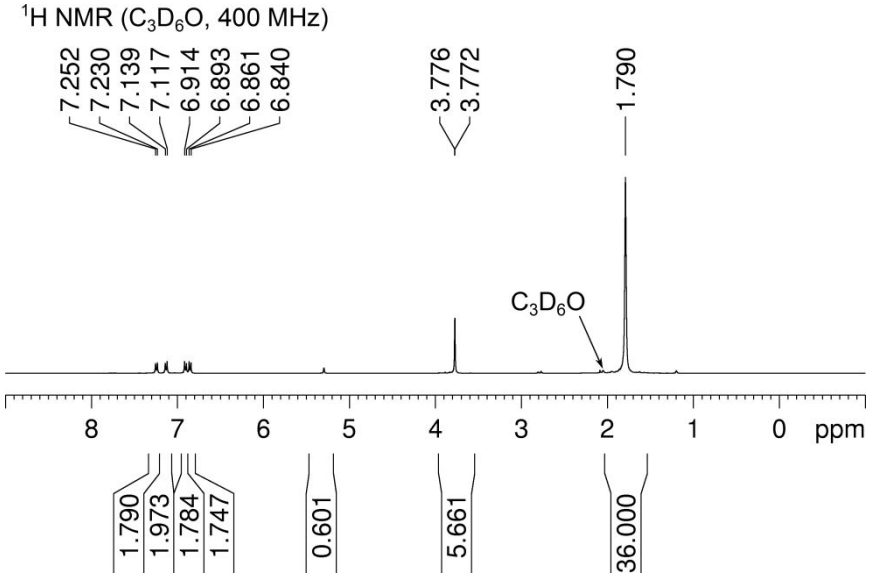

Figure S40. $^{13}C\{^{1}H\}$ NMR spectrum for *trans*-[Ru(=C=CH(C_6H_4-4-OMe))(C≡CC_6H_4-4-OMe)(PMe_3)$_4$]$^+$ BF_4^- **4a** (acetone-d_6, 101 MHz)

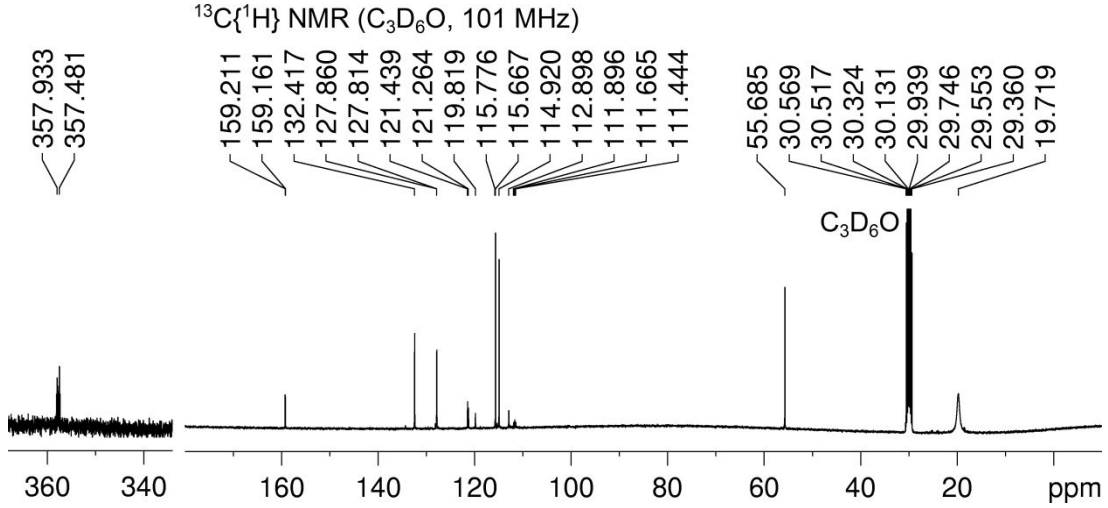

Figure S41. ^{19}F NMR spectrum for *trans*-[Ru(=C=CH(C_6H_4-4-OMe))(C≡CC_6H_4-4-OMe)(PMe_3)$_4$]$^+$ BF_4^- **4a** (acetone-d_6, 565 MHz)

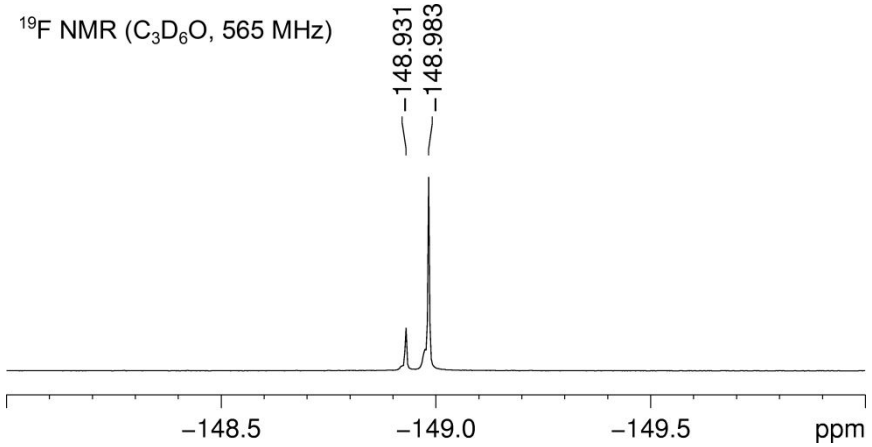

Figure S42. HRMS for *trans*-[Ru(=C=CH(C_6H_4-4-OMe))(C≡CC_6H_4-4-OMe)(PMe_3)$_4$]$^+$ BF_4^- **4a** (acetonitrile, ESI)

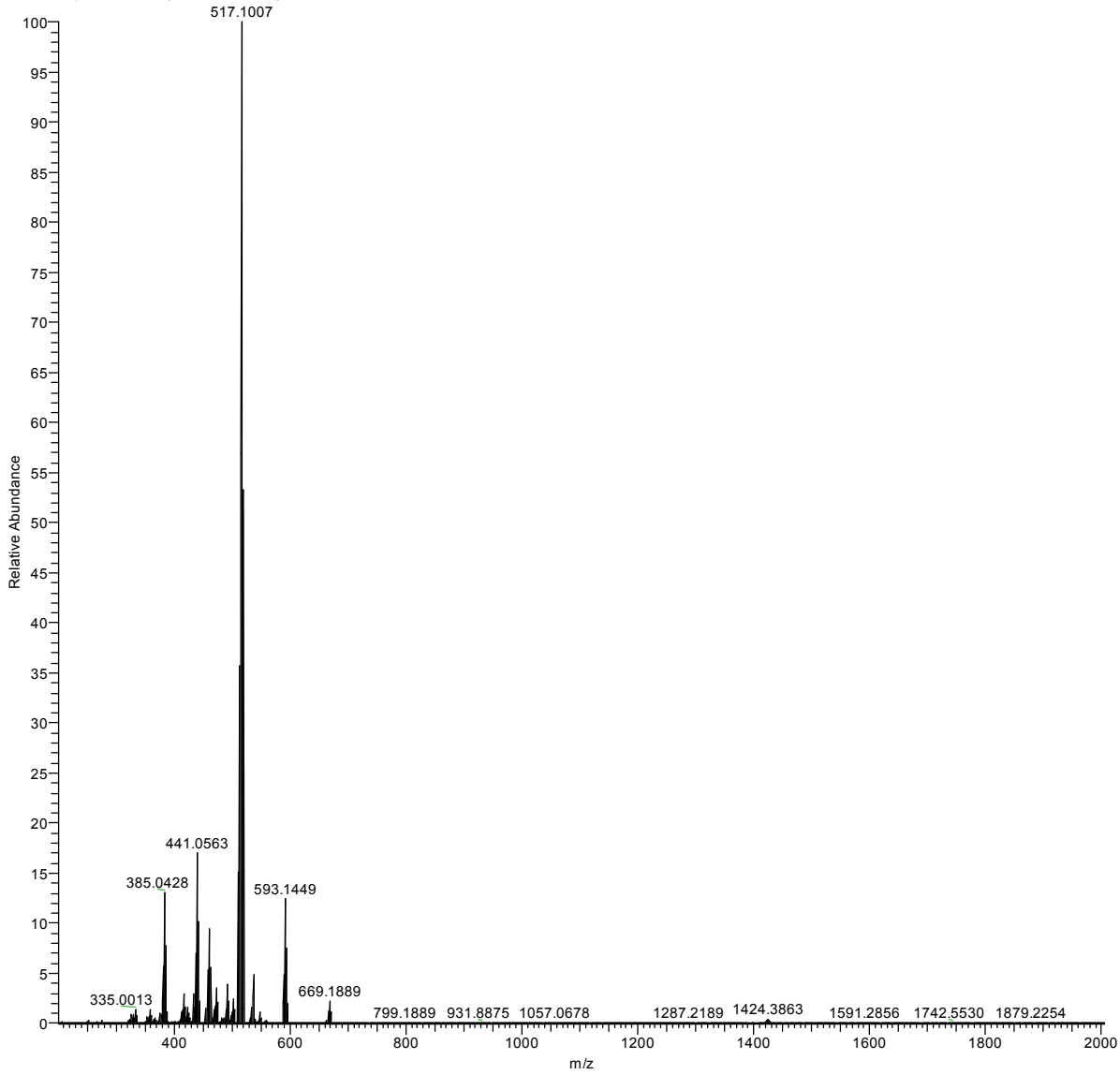

Figure S43. HRMS for *trans*-[Ru(=C=CH(C_6H_4-4-OMe))(C≡CC_6H_4-4-OMe)(PMe_3)$_4$]$^+$ BF_4^- **4a** (expansion, acetonitrile, ESI)

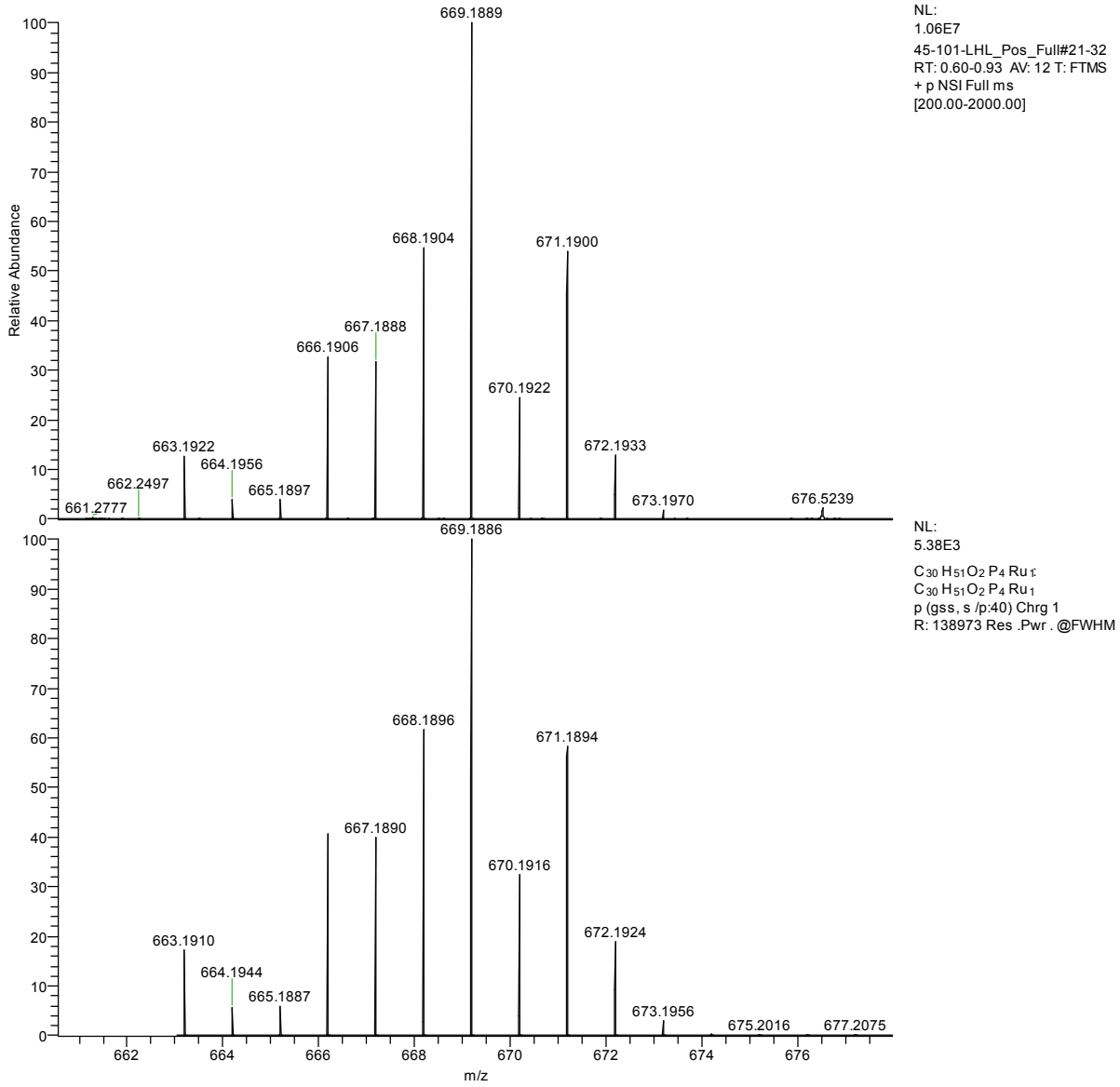

S2.11 ***Trans*-[Ru(=C=CH(Ph))(C≡CPh)(PMe_3)$_4$]$^+$ BF_4^- 4b.**

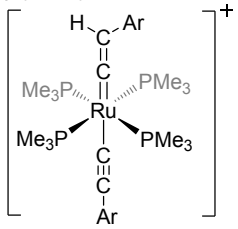

4b: Ar = Ph

Figure S44. $^{31}P\{^1H\}$ NMR spectrum for *trans*-[Ru(=C=CH(Ph))(C≡CPh)(PMe_3)$_4$]$^+$ BF_4^- **4b** (acetone-d_6, 243 MHz)

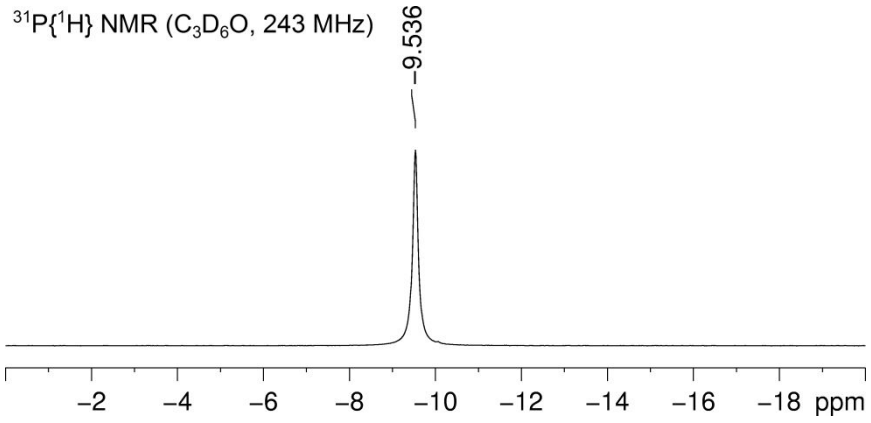

Figure S45. ^1H NMR spectrum for *trans*-[Ru(=C=CH(Ph))(C≡CPh)(PMe_3)$_4$]$^+$ BF_4^- **4b** (acetone-d_6, 600 MHz)

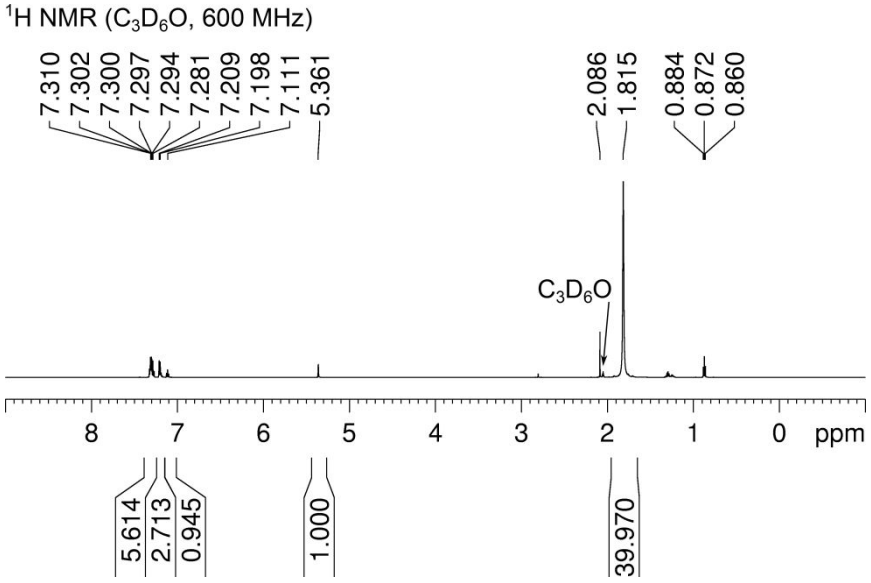

Figure S46. $^{13}C\{^{1}H\}$ NMR spectrum for *trans*-[Ru(=C=CH(Ph))(C≡CPh)$(PMe_3)_4$]$^+$ BF_4^- **4b** (acetone-d_6, 151 MHz)

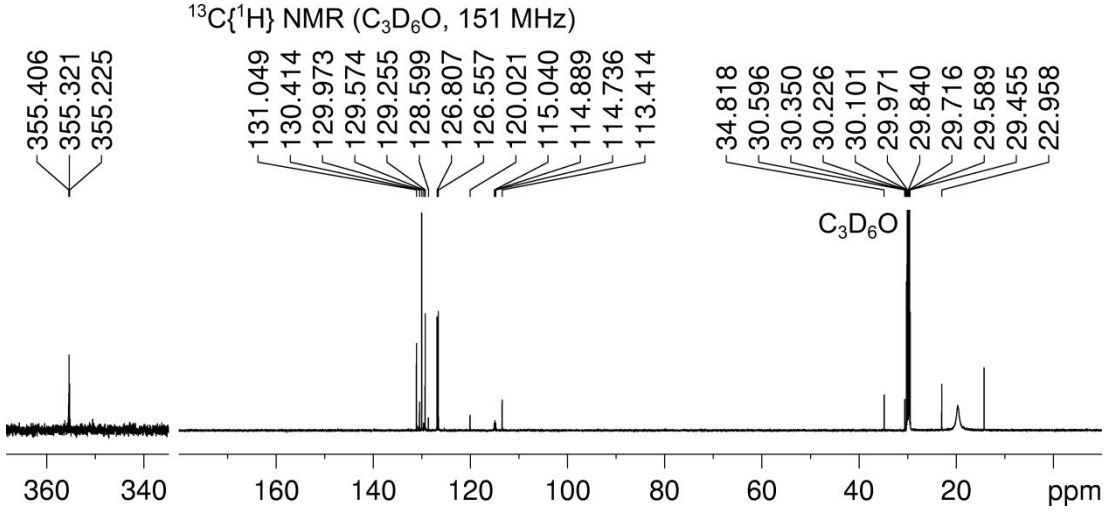

Figure S47. ^{19}F NMR spectrum for *trans*-[Ru(=C=CH(Ph))(C≡CPh)$(PMe_3)_4$]$^+$ BF_4^- **4b** (acetone-d_6, 565 MHz)

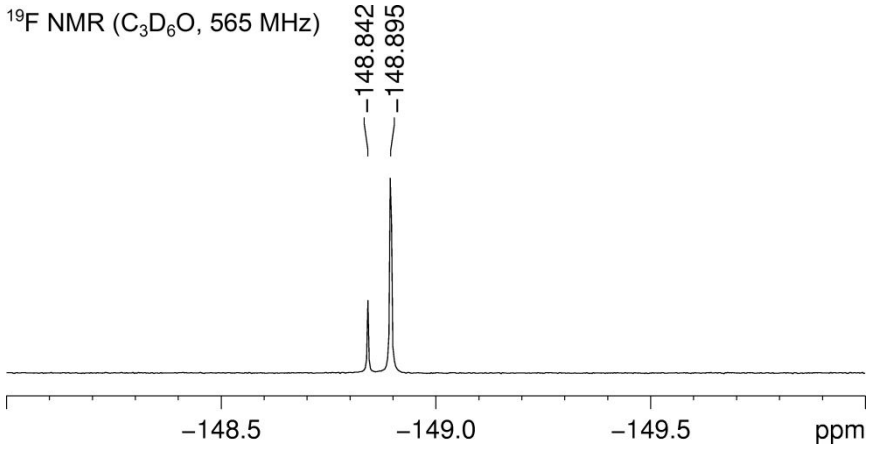

S3 X-ray crystal structure of *trans*-[Ru(=C=CH(C_6H_4-4-OMe))(C≡CC_6H_4-4-OMe)(PMe_3)$_4$]$^+$ BF_4^- 4a

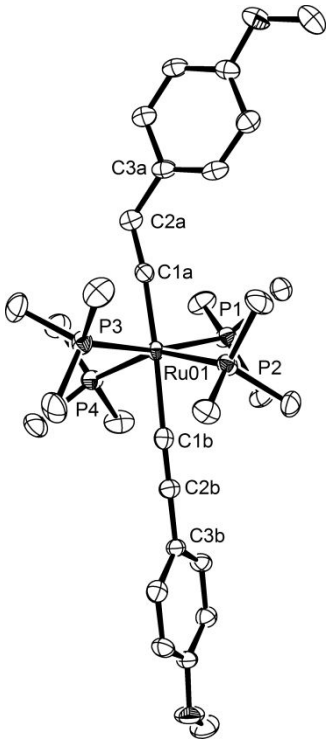

Figure S48. ORTEP plot of *trans*-[Ru(=C=CH(C_6H_4-4-OMe))(C≡C-C_6H_4-4-OMe)(PMe_3)$_4$]$^+$ BF_4^- (**4a**), 50% ellipsoid probability, hydrogen atoms, acetone solvate and BF_4^- counterion have been omitted for clarity. Selected bond lengths (Å) and angles (°): Ru01-P1 2.3744(7), Ru01-P2 2.3984(7), Ru01-P3 2.3699(7), Ru01-P4 2.3647(7), Ru01-C1a 1.881(2), Ru01-C1b 2.086(2), C2a-C1a 1.325(3), C1b-C2b 1.214(3), C2a-C3a 1.476(4), C2b-C3b 1.443(3), C2a-C1a-Ru01 172.5(2), C2b-C1b-Ru01 174.1(2), C1a-C2a-C3a 126.9(3), C1b-C2b-C3b 175.3(3).

Table S1. Crystallographic data for [Ru(η³-CF_3-4-C_6H_4C≡C-C=CH(C_6H_4-4-CF_3))(PMe_3)$_4$]$^+$ BF_4^- (**1c**), [Ru(MeO-4-C_6H_4C≡C-C=CH(C_6H_3-4-OMe)(PMe_3)$_4$] (**2a**), *cis*-[Ru(C≡CC_6H_4-4-CF_3)$_2$(PMe_3)$_4$] (**3c**), *trans*-[Ru(=C=CH(C_6H_4-4-OMe))(C≡C-C_6H_4-4-OMe)(PMe_3)$_4$]$^+$ BF_4^- (**4a**) and *trans*-[Ru(=C=CH(Ph))(C≡CPh)(PMe_3)$_4$]$^+$ BF_4^- (**4b**).

	1c	**2a**	**3c**	**4a**	**4b**
CCDC Number	1966218	1966219	1966220	1966222	1966221
Formula	$C_{30}H_{45}BF_{10}P_4Ru$	$C_{30}H_{50}O_2P_4Ru$	$C_{30}H_{44}F_6P_4Ru$	$C_{33}H_{57}BF_4O_3P_4Ru$	$C_{28.75}H_{48.8}BF_4P_4Ru$
M (g mol^{-1})	831.42	667.65	743.60	813.54	706.23
Size (mm^3)	0.157 × 0.115 × 0.067	0.340 × 0.110 × 0.030	0.217 × 0.074 × 0.052	0.235 × 0.219 × 0.074	0.24 × 0.12 × 0.06
Crystal morphology	Yellow plate	Yellow plate	Colourless plate	Purple plate	Pink plate
Crystal system	orthorhombic	monoclinic	monoclinic	monoclinic	monoclinic
Space group	P21 21 21	P 21/c	P1 21/c 1	P1 21/n 1	P1 21/c 1
a (Å)	10.4300(8)	14.2227(5)	14.201(2)	13.1603(11)	12.6906(9)
b (Å)	14.7049(11)	9.1520(3)	15.580(3)	22.3645(17)	14.1339(10)
c (Å)	24.383(2)	24.9166(8)	17.065(3)	14.1432(11)	22.3102(16)
α (°)	90	90	90	90	90
β (°)	90	98.755(2)	109.975(7)	107.334(2)	98.455(4)
γ (°)	90	90	90	90	90
V (Å^3)	3739.7(5)	3205.51(19)	3548.5(10)	3973.6(5)	3958.2(5)
Z	4	4	4	4	4
D_c (g/cm^3)	1.477	1.383	1.392	1.360	1.185
μ (mm^{-1})	0.660	0.714	0.672	0.605	0.592
F(000)	1696	1400	1528	1696	1465
θ_{max} (°)	24.999	26.20	27.036	27.445	24.999
N	35929	211141	27568	110887	65572
N_{ind}	6580 (R_{int} = 0.1387)	6625 (R_{int} = 0.1448)	7641 (R_{int} = 0.1000)	9127 (R_{int} = 0.0561)	6968 (R_{int} = 0.0788)
Goodness of fit	1.139	1.034	1.009	1.044	1.115
Final R indexes (I >2σ(I))	R_1 = 0.0890 wR_2 = 0.2180	R_1 = 0.0308 wR_2 = 0.0592	R_1 = 0.0690 wR_2 = 0.1649	R_1 = 0.0356 wR_2 = 0.0804	R_1 = 0.0587 wR_2 = 0.1634
Final R indexes (all data)	R_1 = 0.0997 wR_2 = 0.2257	R_1 = 0.0517 wR_2 =0.0671	R_1 = 0.1286 wR_2 = 0.1945	R_1 = 0.0464 wR_2 = 0.0879	R_1 = 0.0771 wR_2 = 0.1788

For structure **3c**, one of the PMe_3 groups and both the CF_3 groups exhibited orientational disorders, which were modelled over two and three (for one of the CF_3 groups) positions with appropriate occupancies. Restrainsts DELU / RIGU/ EADP (as in Shelxl software)[1] were applied wherever necessary to keep the anisotropic displacments of these partially occupied moieties within reasonable limits.

For structure **4b**, the terminal phenyl group atoms of the linear C-C-Ph group showed higher anisotropy; the atoms of this ring were then split over two equally occupied sites. The BF_4 anion was also modelled for disorder with two equally occupied orientations. The geometry of the different parts was restrained to be similar by using command SADI and the anisotropic displacments were restrained by the same commands RIGU and EADP as in **3c**, as per the Shelxl least-squares refinement software.[1]

(1) Sheldrick, G. Crystal structure refinement with SHELXL. *Acta Crystallogr., Sect. C: Cryst. Struct. Commun.* **2015,** *71*, 3-8.